Dear Author,

Please, note that changes made to the HTML content will be added to the article before publication, but are not reflected in this PDF.

Note also that this file should not be used for submitting corrections.

AUTHOR QUERY FORM

ELSEVIER	**Journal: OREGEO** **Article Number: 1322**	**Please e-mail or fax your responses and any corrections to:** **Moorthy, Hemalatha** **E-mail: Corrections.ESCH@elsevier.spitech.com** **Fax: +1 619 699 6721**

Dear Author,

Please check your proof carefully and mark all corrections at the appropriate place in the proof (e.g., by using on-screen annotation in the PDF file) or compile them in a separate list. Note: if you opt to annotate the file with software other than Adobe Reader then please also highlight the appropriate place in the PDF file. To ensure fast publication of your paper please return your corrections within 48 hours.

For correction or revision of any artwork, please consult http://www.elsevier.com/artworkinstructions.

We were unable to process your file(s) fully electronically and have proceeded by

☐ Scanning (parts of) your article ☐ Rekeying (parts of) your article ☐ Scanning the artwork

Any queries or remarks that have arisen during the processing of your manuscript are listed below and highlighted by flags in the proof. Click on the 'Q' link to go to the location in the proof.

Location in article	Query / Remark: click on the Q link to go Please insert your reply or correction at the corresponding line in the proof
Q1	The citation "Martin et al., 1999" has been changed to match the author name/date in the reference list. Please check here and in subsequent occurrences, and correct if necessary.
Q2	The citation "Guillard et al. (1997)" has been changed to match the author name/date in the reference list. Please check here and in subsequent occurrences, and correct if necessary.
Q3	Citation "Bowles et al., 1993" has not been found in the reference list. Please supply full details for this reference.
Q4	The citation "Prospero and Mayol-Bracero (2014)" has been changed to match the author name/date in the reference list. Please check here and in subsequent occurrences, and correct if necessary.
Q5	The citation "Burges, 1911" has been changed to match the author name/date in the reference list. Please check here and in subsequent occurrences, and correct if necessary.
Q6	The citation "Shackleton, 1978" has been changed to match the author name/date in the reference list. Please check here and in subsequent occurrences, and correct if necessary.
Q7	Please check the page range in Ref. Burgess, 1911.
Q8	Please check the page range in Ref. Cabral et al., 2011.
Q9	Please provide an update for reference "Prospero and Mayol-Bracero, in press".
Q10	Please confirm that given names and surnames have been identified correctly. Please check this box if you have no corrections to make to the PDF file. ☐

Thank you for your assistance.

Ore Geology Reviews xxx (2014) xxx–xxx

Contents lists available at ScienceDirect

Ore Geology Reviews

journal homepage: www.elsevier.com/locate/oregeorev

Weathering profile of the Cerro de Maimón VMS deposit (Dominican Republic): textures, mineralogy, gossan evolution and mobility of gold and silver

Q10 E. Andreu [a], L. Torró [a,*], J.A. Proenza [a], C. Domenech [a], A. García-Casco [b], C. Villanova de Benavent [a], C. Chavez [c], J. Espaillat [c,1], J.F. Lewis [d]

[a] Departament de Cristal · lografia, Mineralogia i Dipòsits Minerals, Universitat de Barcelona. C/ Martí i Franquès s/n 08028 Barcelona, Catalonia, Spain
[b] Departamento de Mineralogía y Petrología, Universidad de Granada, Fuentenueva s/n, 18002 Granada, Spain
[c] Corporación Minera Dominicana, C/ José A. Brea Peña #3, Edificio District Tower, Level 3, Ensanche Evaristo Morales, Santo Domingo, Dominican Republic
[d] Department of Earth and Environmental Sciences, George Washington University, Washington, DC 20052, USA

ARTICLE INFO

Article history:
Received 30 May 2014
Received in revised form 4 September 2014
Accepted 11 September 2014
Available online xxxx

Keywords:
Gold
Silver
Iodargyrite
Gossan/leached capping zone
Cerro de Maimón
VMS
Dominican Republic

ABSTRACT

Cerro de Maimón, in the central Dominican Republic, is currently the only VMS deposit under production in the Caribbean region. It is hosted in the Maimón Formation, of early Cretaceous age, which is part of the oldest and chemically most primitive island-arc in the Caribbean. From bottom to top, this deposit can be divided into (i) a primary sulfide zone, (ii) a supergene enrichment zone and (iii) an oxidized zone. This study reports new data on the textural and mineralogical characteristics of the oxidized zone (gossan/leached capping zone) with emphasis in the Au-Ag-bearing phases.

The mineral paragenesis of the oxidized zone is essentially composed of goethite, hematite, quartz and barite. Botryoidal, cellular and brecciated textures can be distinguished. Botryoidal and brecciated textures dominate in the upper parts of the oxidized zone, whereas cellular textures are more common in the intermediate and lower parts. However, the weathering profile is very heterogeneous. The leached capping profile shows evidence of both transported and indigenous gossans. Gold in the oxide paragenesis is extremely pure (99% Au) suggesting that chemical refining took place. Silver occurs mainly as iodargyrite (AgI), and minor AgBr, AgCl, in botryoidal aggregates.

Particles of Au-Ag alloy in the primary mineralization exposed to a weathering environment can be leached and transported by various agents (chemical and biochemical) that may exist simultaneously. In the presence of halides, gold and silver can be leached and transported in a wide range of pH-Eh conditions, especially if iodine is present. Silver is leached more rapidly and over a broader range of pH-Eh conditions, and is preferentially transported as iodine-complexes than other halides.

The presence of iodargyrite in the Cerro de Maimón gossan, fully developed under tropical conditions, suggests that this mineral cannot be considered an indicator of extremely arid environments as typically claimed by many authors; iodargyrite occurrence would rather point to the presence of saline-halide rich groundwater in oxide deposits.

1. Introduction

Since systematic exploration for mineral deposits in the Maimón Formation (central Cordillera, Dominican Republic) began in the late 1970s, several volcanogenic massive sulfide (VMS) occurrences have been discovered within this formation. They include the Cerro de Maimón and Loma Pesada deposits, and Loma Barbuito, Río Sin, Loma la Mina and San Antonio occurrences (Lewis et al., 2000; Nelson et al., 2011).

Cerro de Maimón is a Cu-Zn VMS deposit located 70km northwest of Santo Domingo and 7km east of the town of Maimón in the Monseñor Nouel Province (Fig. 1). Although it was discovered in the 70's as a result of geochemical studies of the gossan outcrops by Falconbridge Dominicana, open pit mining operations did not commence until November 2008. The mine is 100% owned and operated by the Australian company Perilya Limited through its subsidiary Corporación Minera Dominicana (CORMIDOM) (http://www.perilya.com.au/our-business/operations/cerro-de-maimon). The revised resources of the deposit as of December 31st 2013 were 10,642,000

* Corresponding author. Tel.: +34 934021344.
E-mail address: lisardtorro@hotmail.com (L. Torró).
[1] Present address: GoldQuest Mining Corp. 155 Wellington St. W Suite 2920, Toronto, Ontario, M5V 3H1.

http://dx.doi.org/10.1016/j.oregeorev.2014.09.015
0169-1368/© 2014 Published by Elsevier B.V.

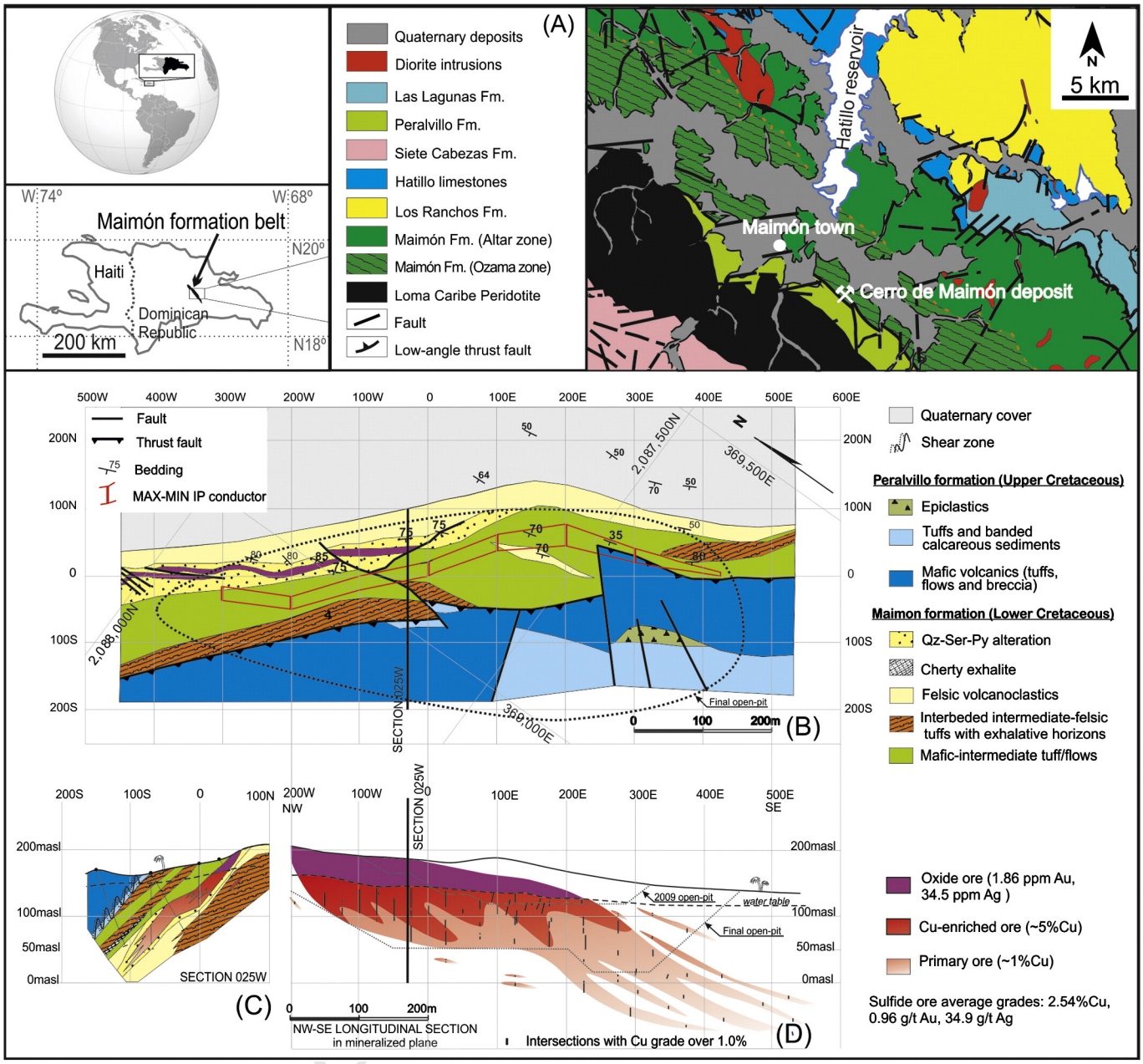

Q1 **Fig. 1.** Geological setting of the deposit and cross sections of the orebody. A: Location map of the deposit of Cerro de Maimón in its geological setting (modified from Martín and Draper, 1999). B: Detailed geological mapping and plan view of the Cerro de Maimón orebody as shown by Induced Polarity (IP) geophysical survey. C: Detailed N-S cross section of the orebody and the host formations. D: Detailed cross section in mineralized plane of the orebody, projected in NW-SE trend. Several low-grade sulfide fringes are detected in the SE ending of the orebody that have been interpreted as the stockwork or feeding zone of the sulfide lens.

tonnes of sulfide ore averaging 1.47% Cu, 0.78 g/t Au, 26.01g/t Ag and 1.49% Zn, and 545,000 tonnes of oxide ore averaging 1.04 g/t Au and 11.80g/t Ag. Two types of ore are processed, (i) the sulfide ore, for the production of Cu-concentrates (with Au-Ag as byproducts) through a classical flotation process and (ii) the oxide ore, for recovering Au-Ag *doré* bars by cyanide leaching and Merrill-Crowe precipitation. The Cerro de Maimón Mine Plant process 1,300 tpd sulfides ore and 700 tpd oxide ore for a yearly production of approximately 12,000 tonnes of copper concentrate, 12,000 ounces of gold and 325,000 ounces of silver.

Although Cerro de Maimón is the only VMS deposit currently under production in the Caribbean realm, only a few detailed studies have been published. The first studies of the deposit and the sulfide mineralization carried out by Watkins (1990) and Astacio et al. (2000) were followed by a summary of the structure, petrography, whole rock and oxygen isotope geochemistry by Lewis et al. (2000). However, no published data of the oxidized zone (referred to as gossan or leached capping in this contribution) from this VMS exists beyond some short communications (Andreu et al., 2010; Colomer et al., 2013). The main portion of the oxidation zone covering the Cerro de Maimón deposit has already been mined out and stored away, allowing its simultaneous mineral processing with the underlying massive sulfide body ores. Therefore, the samples here studied represent a highly valuable in-situ collection of material from this oxidized zone.

Gold and silver enrichment is well documented in leached capping zones overlying supergene and primary (hypogene) sulfide assemblages. However, the factor causing the silver halides to precipitate are still being debated (e.g. Izawa et al., 2010; Pekov et al., 2011; Sillitoe, 2009; Taylor, 2011). To be noted is that Ag halides (especially iodargyrite), are commonly proposed as mineral indicators of arid or

Please cite this article as: Andreu, E., et al., Weathering profile of the Cerro de Maimón VMS deposit (Dominican Republic): textures, mineralogy, gossan evolution and mobility of..., Ore Geol. Rev. (2014), http://dx.doi.org/10.1016/j.oregeorev.2014.09.015

semi-arid climatic conditions in which halides are common in the ground waters (e.g. Boyle, 1997; Reich et al., 2009).

In this paper, we report the results of a detailed study of the structure, textures, mineralogy and composition of gold and silver phases of the oxidized ore zone at Cerro de Maimón VMS deposit. The data are used to constrain the mechanisms of supergene enrichment and behavior of gold and silver during the weathering process in the Cerro de Maimón gossan and other similar deposits.

2. Geological setting

2.1. Regional geology

The geology of the island of Hispaniola (Haiti and the Dominican Republic), resulted largely from the Cretaceous-Tertiary oblique convergence and underthrusting of the North American Plate beneath the Circum-Caribbean island-arc. Subduction and related arc magmatism ceased in the middle Eocene with the collision of the arc with the Bahamas Platform (Lewis and Draper, 1990; Mann et al., 1991; Pérez-Estaún et al., 2007). During the Oligocene, a change in the stress regime along the Northern Caribbean Plate Boundary Zone (NCPBZ) gave rise in the Oligocene to transform movement and strike-slip faulting parallel to the NCPBZ. This activity along the NCPBZ continues today, particularly in Hispaniola (Mann et al., 1991).

The late Early Cretaceous–Eocene Circum-Caribbean island-arc system is a complex collage of oceanic and intra-oceanic volcanic arc units (Pindell and Barrett, 1990). The formation of the ore deposits in the Greater Antilles, including those related to continental margins, oceanic basins and volcanic arc settings, was discussed by Nelson et al. (2011) within the framework of the tectonic evolution of the northern Caribbean.

The Cerro de Maimón deposit is hosted by the Maimón Formation (Lewis et al., 2000). This formation, together with Los Ranchos and Amina Formations., is part of the oldest and chemically most primitive island-arc volcanism in the Caribbean region (Escuder-Viruete et al., 2007a, 2009; Lewis and Draper, 1990; Lewis et al., 2002; Nelson et al., 2011). The Maimón Formation is a 9 km wide and about 73 km long NW-SE trending belt (Fig. 1a) which can be divided into two structural provinces aligned parallel to the trend of the belt: (i) the Ozama shear zone to the SW, whose extreme deformation has obliterated most of the original igneous textures, and (ii) the much less deformed Altar Zone to the NE (Draper et al., 1996; Lewis et al., 2000). Both zones have been metamorphosed to greenschist facies.

The Maimón Formation is bounded tectonically by the Loma Caribe peridotite and the Peralvillo Sur Formation (Escuder-Viruete et al., 2007b; Lewis et al., 2002) to the southwest and the Los Ranchos Formation to the northeast (Fig. 1a). Draper et al. (1996) suggested that the Loma Caribe peridotite, a serpentinized harzburgite with minor dunites, lherzolites and pyroxenites forming part of a dismembered ophiolite complex (Lewis et al., 2006; Proenza et al., 2007), was tectonically emplaced over the Maimón Formation during the late Albian as a consequence of a mid-Cretaceous event of subduction polarity reversal. The obduction of the peridotite body along a northward thrust resulted in deformation and metamorphism of the Maimón Formation, particularly in the Ozama shear zone. The Loma Caribe peridotite belt is separated from the Maimón Formation at their southern contact by the Peralvillo Sur Formation, a thin sequence of arc-related volcanic and volcano-sedimentary rocks of apparent Late Cretaceous age (Lewis et al., 2000; Martín and Draper, 1999), documenting further tectonic movements of late Cretaceous-Tertiary age. The Maimón, Amina and Los Ranchos Formations are overlain by the Hatillo limestone, a massive micritic sequence deposited under shallow-water, reefal conditions during the Albian to Cenomanian (Kesler et al., 2005). However, the Maimón Formation overthrusts the Hatillo limestone along the Hatillo Thrust. Both Maimón and Hatillo Formations are intruded by diorites of apparent Paleocene age (Bowin, 1966; Martín and Draper, 1999).

The Maimón Formation is composed of low-grade metamorphosed and variably deformed pre-Albian bimodal volcanic and volcaniclastic rocks containing scarce horizons of breccias and conglomerates. A belt of well-laminated rocks of sedimentary origin that is conformable with the volcanic sequence crops out in the north central part of the Maimón Formation. These are mainly fine-grained meta-tuffs but cherts, dark shales and limestones are present (Kesler et al., 1991; Lewis et al., 2000). Geochemically, the mafic (basaltic) rocks range from low-Ti tholeiites with boninitic affinities to typical oceanic island-arc tholeiites. Felsic rocks are quartz-feldspar tuffs and porphyries that exhibit a similar depleted trace element signature indicating a common source (Escuder-Viruete et al., 2007a; Lewis et al., 2000, 2002).

The protoliths of the Maimón, Amina and Los Ranchos Formations have very similar elemental and isotopic signatures, suggesting common magma sources and petrogenetic processes (Escuder-Viruete et al., 2007a; Horan, 1995; Lewis et al., 2002). The origin and relative position of these units within the primitive island-arc is still a matter of debate. Escuder-Viruete et al. (2007a) suggested a cogenetic origin for the three Formations. In contrast, Lewis et al. (2000) distinguished a fore-arc setting origin for the Maimón and Amina Formations and an axial island-arc context for the Los Ranchos Formation. On the other hand, Horan (1995) concluded that the Maimón Formation formed in a back-arc basin. Lead isotope ratios of the Maimón and Amina Formations are lower $^{206}Pb/^{204}Pb$ (~18.4), $^{207}Pb/^{204}Pb$ (~15.5) and $^{208}Pb/^{204}Pb$ (~37.9) than those of the Los Ranchos Formation (Horan, 1995). The fact that the Maimón and Amina Formations mainly host exhalative deposits in contrast to the epithermal character of those hosted by the Los Ranchos Formation suggests that they formed in different environments within a backarc-arc-forearc setting.

2.2. Geology of the deposit

The Cerro de Maimón deposit is located in the Ozama shear zone, in the southern branch of the Maimón Formation, very close to the thrust-faulted contact with the Peralvillo Formation (Fig. 1a). Intense deformation, metamorphism and pervasive hydrothermal alteration (especially recorded in the foot wall rocks) have largely destroyed the original features of the igneous rocks. Based on the least altered lithologies, the protoliths of the host rocks were described as mafic to intermediate submarine volcaniclastic and volcanic rocks by Lewis et al. (2000). Quartz-sericite-pyrite schists are the dominant foot wall rocks, grading to chlorite-quartz-feldspathic schists at depth. Two lithologies grading to one another dominate in the hanging wall: i) pale epidote-bearing mafic schists spotted with chlorite flakes and ii) dark green chlorite schists with prominent calcite-quartz veins (Lewis et al., 2000). Thin graphitic and hematitic chert horizons are described to be more developed in the western hanging wall (Watkins, 1990). The high concentration of quartz veins associated with a strong hydrothermal alteration in the westernmost area led Lewis et al. (2000) to the conclusion that the western foot wall zone could correspond to a sulfide stockwork whereas the eastern foot wall rocks would be distal to the feeding zone.

The ore-body lens is 1000 m long, about 300 m wide and 15 m thick on average although the thickness reaches up to 40 m locally. The orebody dips 40° to the southwest with a general steepening of the dip to the northwest and it flattens southeast to 20° down plunge (Watkins, 1990) (Fig. 1b). The deposit can be broadly separated, from bottom to top, into (Fig. 1c): i) the primary mineralization with a Cu-Zn ratio that tends to 1:1 in depth and mainly composed of pyrite, chalcopyrite and sphalerite (Colomer et al., 2013); ii) an irregular cementation or supergene enrichment zone with up to 10 % Cu grades and a Cu-Zn ratio of 3:1, containing secondary copper sulfides consisting of a micron-sized intergrowth of chalcocite and covellite along with djurleite, digenite or yarrowite; and iii) a mushroom-like shaped oxidized zone (gossan/leached capping zone). Considering its ore composition, the Cerro de Maimón deposit is clearly a Cu-Zn type, and based on

Please cite this article as: Andreu, E., et al., Weathering profile of the Cerro de Maimón VMS deposit (Dominican Republic): textures, mineralogy, gossan evolution and mobility of..., Ore Geol. Rev. (2014), http://dx.doi.org/10.1016/j.oregeorev.2014.09.015

its host rocks, alteration assemblages and tectonic setting it can be mainly classified as a bimodal mafic-dominant deposit (Nelson et al., 2011) according to Franklin et al. (2005) VMS classification.

Gold and silver grades are mostly constant along the primary sulfide body and the cementation zone. Detailed study of the mineralogy of ores in these zones allowed the detection of very scarce electrum with Au contents slightly higher than those of Ag; electrum grains, with sizes around 15microns, were systematically detected in those domains of the massive sulfide body registering higher deformation and metamorphism (e.g. rotation of pyrite grains with adjacent pressure shadows) so a metamorphic origin is proposed for electrum. As far as Au-bearing phases were not observed in the samples of most of the primary sulfide body, it is interpreted to occur as micro-inclusions within pyrite (invisible gold). Rounded silver-telluride (mainly hessite) grains of a few tens of microns in size appear scattered in most of the samples; however, they are concentrated along tennantite margins with textural evidences indicating that they would have formed principally from alteration of the last. Silver contents in tennantite crystals is up to 3.48 wt. %.

3. Sampling and Analytical Techniques

The weathering profile was vertically sampled in the open pit during the summer 2009. Gossan samples were collected from 10 mine benches (from bench 195 to bench 150) in order to study the vertical distribution of textures and mineralogy. All the analytical work was carried out at the Centres Científics i Tecnològics of the University of Barcelona. Powder X-ray diffraction (XRD), Scanning Electron Microscopy coupled with energy dispersive spectrometry (SEM-EDS) and Electron Microprobe (EMP) analyses were combined to characterize the mineralogy.

The mineralogy was first studied with XRD using a Panalytical X'Pert PRO MPD X-ray diffractometer with monochromatized incident Cu-Kα1 radiation at 45 kV and 40 mA, equipped with a PS detector with an amplitude of 3°. Diffraction patterns were obtained by scanning powders from 4° to 80° (2θ) on samples crushed in an agate mortar to a particle size <30 μm. Analytical conditions were a scan time of 50 seconds at a step size of 0.0170° (2θ). The software used for the interpretation of the diffraction patterns was Panalytical High Score Plus v2.2b.

A total of 20 polished sections of the gossan were studied by reflected light microscopy. Morphological, textural and preliminary compositional features of the selected samples were studied by SEM-EDS using an Environmental SEM Quanta 200 FEI, XTE 325/D8395 equipped with an INCA Energy 250 EDS microanalysis system. Operating conditions were an acceleration voltage of 20 kV and 5 nA.

Gold and silver-bearing phases were analyzed using a four-channel Cameca SX50 electron microprobe (EMP) with wavelength dispersive spectrometry (WDS). Analyses were performed at 20 kV accelerating voltage, 20 nA beam current, 2 μm beam diameter and counting time of 10 seconds per element. The routine used for the analysis of halides was 15 kV and 6 nA. Calibrations were performed using the following natural and synthetic standards: FeS_2 (Fe, S), Cu_2S (Cu), GaAs (As), ZnS (Zn), metallic Ni (Ni), metallic Au (Au), metallic Co (Co), HgS (Hg), AgS_2 (Ag), PbS (Pb), AgCl (Cl), KBr (K) and CsI (I).

Finally, predominance Eh-pH diagrams of the Ag/Au-Cl-Br-I-H_2O and Fe systems were calculated using "MEDUSA" code and "HYDRA" database (Puigdomènech, 2010).

4. Structure of the gossan profile at Cerro de Maimón deposit

The weathering profile at Cerro de Maimón (Fig. 2) shows many similarities to common models of sulfide oxidation as those described by Blain and Andrew (1977), Taylor and Thornber (1992), Thornber and Taylor (1992), Scott et al. (2001), Belogub et al. (2008) or Velasco et al. (2013) gossans in the Iberian Pyrite Belt, with the exception of Las Cruces gossan as stated by Yesares et al. (2014). The general profile of the oxidized ore at Cerro de Maimón presents a well-developed surficial gossan/leached capping and minor (often inexistent) leached zones represented by pyrite-quartz sands (Fig. 2). Despite the general trends shown in Fig. 2A, different oxide lithofacies appear at the same level, since textural features are heterogeneously distributed (Fig. 2B).

The oxidized zone is composed largely of variable proportions of massive, brecciated, cellular box-work and massive botryoidal-textured goethite/hematite rocks, examples of which are shown in Figs. 2A, 3A and B.

The upper part of the profile is dominated by breccias (Fig. 3C) and massive botryoidal goethite aggregates cementing residual silica and barite (Fig. 3B). Earthy microbreccias are found along the entire profile as a result of dissolution-collapse processes, but they are more frequently observed in the upper part of the profile. Hematite is dominant in the upper part of the profile.

The central and lower parts of the gossan are dominated by goethitic cellular boxwork layers (Fig. 2A). Related to schistose fabrics of the host rock, cavernous layers (Fig. 3D) with geopetal stalactitic structures (Fig. 3E) are found in the central and basal parts of the profile. These open cavities are similar to those described in Minas Carlota, Cuba (Hill, 1958) and in the Rio Tinto district (Velasco et al., 2013). These structures consist of botryoidal aggregates of oxyhydroxides with a fluidal-gel appearance partially infilling the caverns that locally appear in contact with layers of fine goethite mud.

The lowermost levels of the profile are characterized by the presence of fine-grained goethitic mud in clayey and humid layers showing an intense yellow-mustard color (Figs. 2A, 3F and G). Similar layered structures have been reported in other localities as a yellow wet layer at Mina Margot, Cuba (Hill, 1958) and Cyprus (Bruce, 1948) and as a precious metal layered structure at Rio Tinto (Williams, 1950) and Filón Sur Tharsis (Capitán et al, 2003). Indeed, mud-goethite layers seem to be closely related to gold precipitation since they return the highest Au grades of the ore (around 15 g/t in average according to mine working reports).

The oxide-sulfide contact, as exposed in 2009, was defined by irregular leached and supergene enrichment zones (Fig. 2B) indicating an oscillating water table which would have controlled the oxidation-reduction processes. As a result of the leaching process, the upper part of the sulfide zone consists of a friable granular quartz-pyrite layer. In this zone, Cu-sulfides have been leached by percolating waters resulting in a 1–4 m thick Cu-poor layer in which only pyrite and quartz remain. Similar leached layers are described in weathering profiles of VMS deposits from the South Urals (Belogub et al., 2008), at Flin Flon deposit (Brownell and Kinkel, 1935), in Bathrust Mining camp (Boyle, 1994) and in Las Cruces (Yesares et al., 2014). Below the leached zone, copper rich waters precipitated in the cementation zone (*i.e.* supergene enrichment zone). Cu-rich waters replaced other sulfides increasing the copper grade. The thickness of the supergene enriched zone is up to 60 m. The distribution and contact of the oxidized and the supergene enriched areas are in addition controlled by fractures through which rainwater and groundwater percolated down to 120 m depth; locally, tongues of gossan material penetrating vertically into the massive sulfide body with sharp contacts were observed along fractures following the direction of regional schistosity (Fig. 4).

According to the general oxidation model for VMS deposits (Taylor and Thornber, 1992), Cu-carbonate and Cu-sulfate zones appear at the oxide-sulfide interface. However, at Cerro de Maimón, these layers are poorly developed. Malachite only appears as millimeter-sized veins in fractures or local shear zones within the chlorite schists. Chalcanthite is observed as efflorescence on the exposed walls of mine workings in the uppermost sulfide zone, crystallized from mine waters (Figs. 2A and 3H).

Iron oxyhydroxides precipitates along open fractures such as cracks and joints are observed in the wall rocks (Fig. 3I).

Please cite this article as: Andreu, E., et al., Weathering profile of the Cerro de Maimón VMS deposit (Dominican Republic): textures, mineralogy, gossan evolution and mobility of..., Ore Geol. Rev. (2014), http://dx.doi.org/10.1016/j.oregeorev.2014.09.015

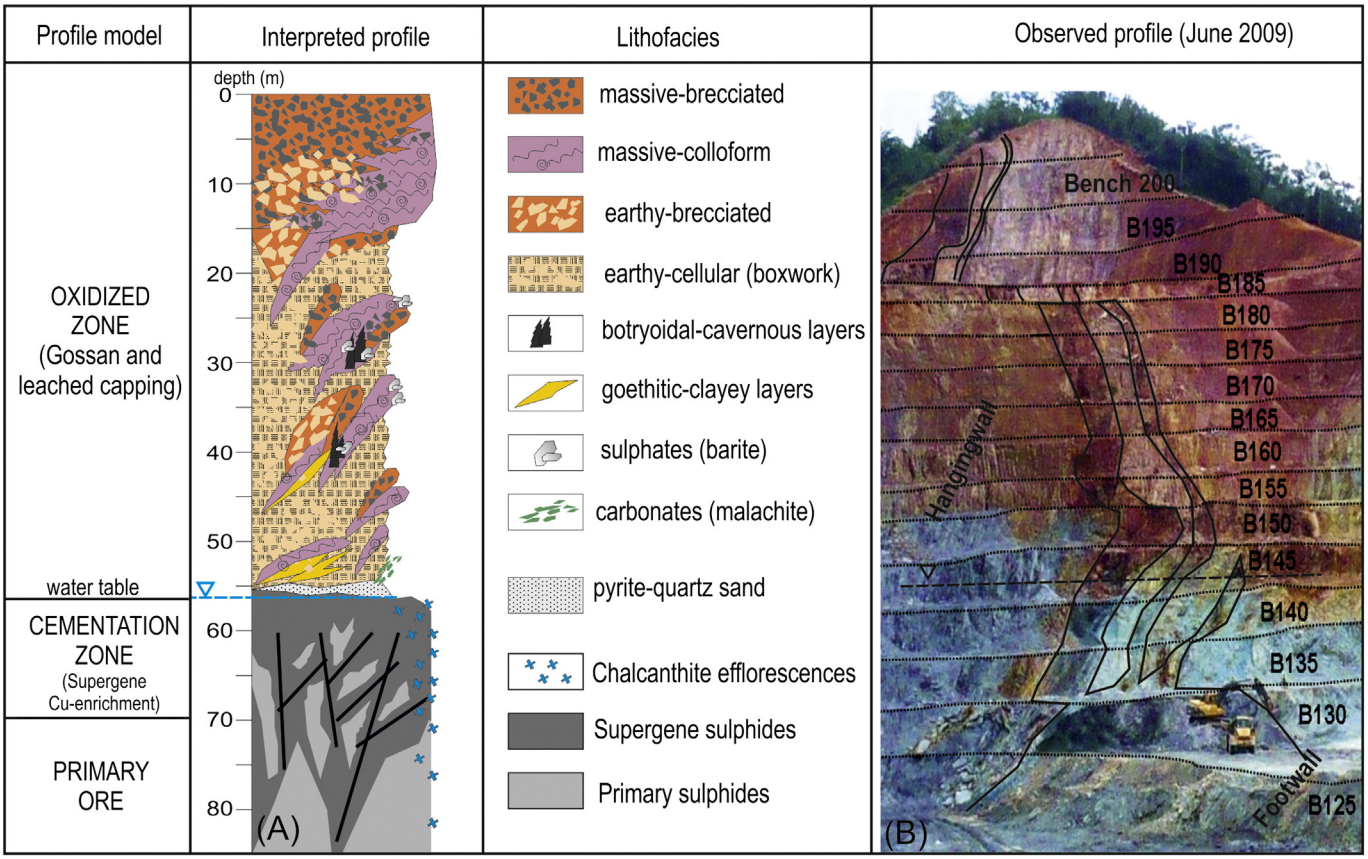

Fig. 2. Weathering profile and field photograph of the orebody as it appeared during Spring 2009. A: Schematic weathering profile of the Cerro de Maimón orebody. Note that the oxide body or gossan zone is composed by successive lithofacies evolving from the uppermost mature facies (massive) to immature earthy-cellular facies, and goethitic-clayey layered structures in the lowermost part of the oxide body as the last stages of gossan formation. A pyrite-quartz sandy level is observed in the contact with the sulfide enrichment zone, representing the leaching zone. Sulfides appear at approximately 45 m under the surface, showing chalcanthite efflorescences when exposed during mining works. The whole profile is strongly subordinated to the previous schistose structure. B: Field photograph of the open-pit showing the steep position of the massive lenses and the schistose character of the formation. Note the bluish chalcanthite efflorescences of the sulfide zone. Each bench is 5 m high and the number indicates meters above sea level (m.a.s.l.). Benches 200–185 appear in a backward plan of view.

5. Textures and mineralogy in the oxide zone

In general, the mineral paragenesis of the oxide ore can be described as a goethite-hematite assemblage with minor variable quantities of barite, silica and scarce layers of secondary minerals such as kaolinite, celadonite and gibbsite. Three groups of textures have been distinguished under the optical microscope: i) cellular-boxwork, ii) microbreccias, and iii) botryoidal-colloform.

Cellular or boxwork textures consist of a limonite-cemented sponge hosting quartz and barite fragments showing evidences of *in situ* formation. Samples show cubic goethite phantoms as a result of the oxidation and leaching of the former sulfides, developing box- and ladder-work textures with different grades of oxide-cementation and porosity (Fig. 5A and B).

Brecciated textures consist of quartz and/or barite fragments cemented by variable amounts of iron oxyhydroxides, resulting in different grades of rock friability and porosity (Fig. 5C and D). Observed gradations would suggest that box-work textures may evolve to *in situ* breccias as a result of solution, volume reduction, compaction and cementation (Laznicka, 1988, 1989; Velasco et al, 2013). In general, cellular and brecciated textures are characterized by high porosity (up to 50 % vol.).

Botryoidal aggregates are composed of successive layers of goethite and hematite developed over cores of gangue minerals and infilling voids. Porosity within botryoidal zones appears as residual voids among aggregates, as long and thin (up to 20 μm) spaces between botryoidal-laminated aggregates or as shrinkage cracks (Fig. 5E and F). A continuous spectrum exists between botryoidal and brecciated zones. Microfacies range from clast-supported fabrics (cemented by colloform aggregates) where the gangue minerals dominate (silica, barite) to matrix-supported fabrics with massive colloform zones where gangue only represents the nucleation cores.

Multiple episodes of goethite-hematite precipitation can be distinguished by examination of the samples under the optical microscope, especially within the botryoidal-massive assemblages (Figs. 5E and F). In addition, a common feature in most of the studied samples is an outer rim of hematite around botryoidal goethite aggregates (Fig. 5G and H), as observed by Velasco et al. (2013) in the Rio Tinto gossan. Goethite is much more abundant than hematite at the deposit scale, though hematite is more abundant in the uppermost zone samples.

Ore minerals in the oxide zone are mainly native gold (Au) and Ag-halides (mostly AgI as explained in Section 6) (Figs. 6 and 7). Gold is observed as minute (from 1 to 10 μm) rounded, often reniform-shaped grains. Gold grains appear in voids within botryoidal aggregates of goethite-hematite (Fig. 6B, D and F), and are especially abundant in goethitic-mud layers (Fig. 6A and C); in those layers, gold appears as clusters of several rounded grains in contact with shrinkage cracks (Fig. 6A). Gold grains found in colloform goethite appear filling pores (Fig. 6B). The presence of Ag-halides is also closely related to botryoidal aggregates (Fig. 7). They occur as anhedral grains filling voids inside botryoidal aggregates, often fitting the shape of the pores (Fig. 7D, E and F). These phases are also observed as euhedral grains inside voids of botryoidal goethite (Fig. 7C) or as tiny sparks scattered in the sulfide box-work pores (Fig. 7A). Some grains show compositional zoning, with

Please cite this article as: Andreu, E., et al., Weathering profile of the Cerro de Maimón VMS deposit (Dominican Republic): textures, mineralogy, gossan evolution and mobility of..., Ore Geol. Rev. (2014), http://dx.doi.org/10.1016/j.oregeorev.2014.09.015

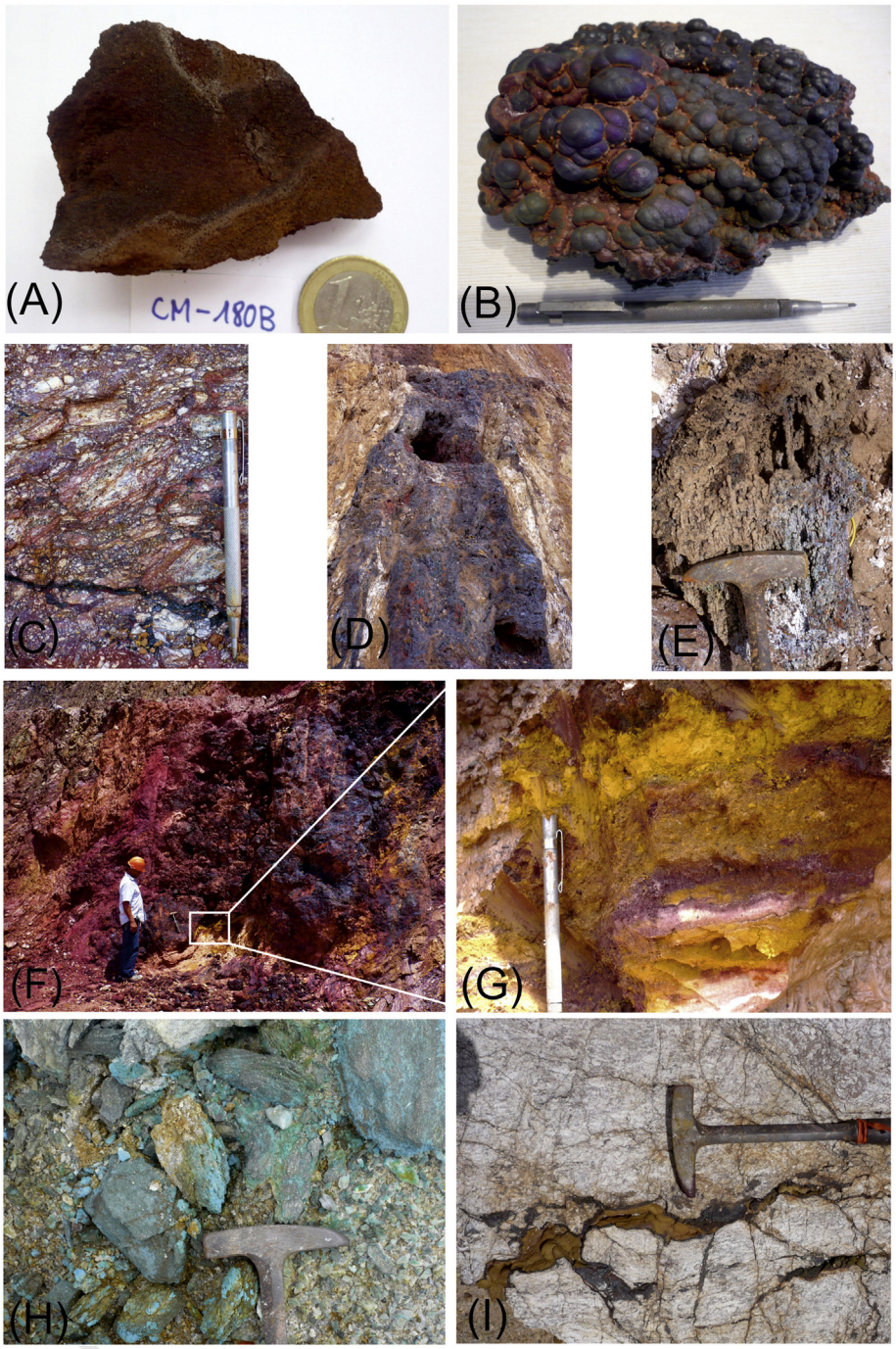

Fig. 3. Hand specimens and field photographs showing representative structures and lithofacies observed along the Cerro de Maimón weathering profile. A: Friable-sandy sample showing red-brown shades corresponding to oxide precipitation fronts. Reddish areas correspond to goethite dominated areas while dark-brown area corresponds to hematite-goethite suggesting hematite-formation fronts. Microscopic observation of the sample determined a cellular lithofacies with different degrees of cementation. B: Massive-botryoidal hand specimen showing the typical colloform iron oxyhydroxide aggregates with tiny barite crystals on them. C: Massive-brecciated lithofacies suggesting collapse-cementation processes. D: Cavernous voids in the massive-oxide layer. Note the mylonitic structure of the lens. The massive layer is around 60 cm wide. E: Oxide sample showing columnar geopetal structures. Some of the cavernous voids were partially filled by such structures. F: Picture corresponding to the base of the main oxide lens (bench 145) showing massive oxides and the thickest clayey-goethitic layers. G: Detail of the clayey, mustard-colored goethitic layer. AAS analysis carried out during mining works reported gold grades up to 33.2 g/t (15 g/t in average). H: Chalcanthite efflorescences observed over exposed sulfides. This observation explains the handicaps encountered during the Cu-flotation process since the existing Cu^{2+} activates the sphalerite surface and reduces the Cu-concentrate purity. I: Weathered sericitic schist outside the confines of the oxide orebody showing open fractures coated and cemented by oxides, evidence of fracture-driven transport and precipitation.

an iodine-rich core and progressive depletion in this element towards rims (Fig. 7A and B). Ag-halides also appear as rubbly sub-rounded to angular fragments cemented by a limonitic matrix together with barite and quartz fragments (Fig. 7G, H and I). Grain size of Ag-halides is heterogeneous, typically ranging from 5 to 15 μm, although 100 μm-sized grains are observed.

Identified clay minerals include kaolinite, illite and celadonite. Kaolinite was mainly observed in the upper part of the profile as

Please cite this article as: Andreu, E., et al., Weathering profile of the Cerro de Maimón VMS deposit (Dominican Republic): textures, mineralogy, gossan evolution and mobility of..., Ore Geol. Rev. (2014), http://dx.doi.org/10.1016/j.oregeorev.2014.09.015

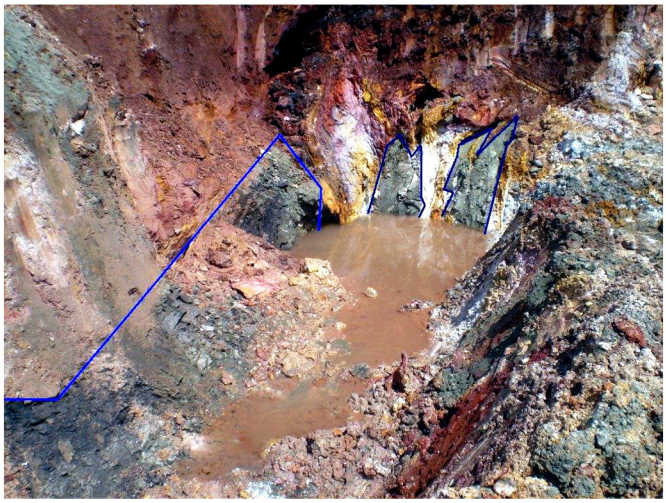

Fig. 4. Photograph taken in 2006 at the beginning of mining of the face of the oxide zone that shows the nature of the contact between the oxide and the zone of supergene enrichment and sulfides. Tongues of gossan material penetrate vertically into the sulfide.

botryoidal gold-bearing layers coating limonitic botryoidal aggregates (Fig. 6E). Jarosite, and other common minerals found in oxidation profiles such as lepidocrocite, have not been found at Cerro de Maimón.

6. Mineral chemistry

A summary of the composition of Au- and Ag-bearing minerals analyzed by EMP is given in Table 1.

Analyzed native gold grains are extremely pure, with Au concentrations systematically above 96 at.% with an average of 99.4 at.%. Ag contents are remarkably low for all the analyzed Au grains, normally below the detection limit, and only compositions up to 0.26 at.% were obtained. Iron concentrations are also usually below the detection limit; anomalous high Fe values, up to 3.6 at.%, are interpreted as interferences with the surrounding limonitic phases. The amounts of Cu and Hg are below the detection limits.

Identified Ag-bearing minerals from the Cerro de Maimón gossan are exclusively halides with variable contents of Cl, Br and I (Table 1). The spongy texture of these phases represented a problem when analyzing them by EMP, limiting the number of acceptable analyses returned. Fig. 8 shows the normalized microprobe results (at.%) of the analyzed Ag-halides plotted in a triangular diagram with the Cl-Br-I end-members (chlorargyrite, bromargyrite and iodargyrite respectively) in the edges. Two distinct clusters are evident, one of them closely lying in the iodargyrite edge with chlorine and bromine practically absent (Cl:Br:I = 0.5:0.5:99.0); the other cluster, in which iodine is much less abundant, is more diverse, with a Cl:Br:I ratio averages of 37.5:50.7:11.8.

According to the EMP results, the analyzed Ag-halides at Cerro de Maimón are iodargyrite and Cl-Br-I Ag-halides. Although apparently there is limited solid solution between chlorargyrite and iodargyrite and between bromargyrite and iodargyrite, a complete solid solution between the chlorargyrite and bromargyrite is described (Boyle, 1997). This group of minerals is frequently grouped under the name of "embolite". Thus, Cl-Br-I Ag-halide phases here described, especially those with lower I contents, can be classified under the name "embolite".

Analyses of the compositions of Ag-halides from the Ag-Pb-Zn Broken Hill deposit reported by Gillard et al. (1997) are also plotted in Fig. 8. As in the case of Cerro de Maimón, Ag-halides from Broken Hill mainly plot in two separated compositional fields, one extremely I-rich (iodargyrite end-member) and the other I-poor (embolites). However, the embolite specimens from Broken Hill are poorer in I and richer in Cl than those analyzed from Cerro de Maimón gossan.

7. Discussion

7.1. Indigenous vs. transported

In general, gossans and oxidized outcrops can be classified into indigenous, transported and exotic (Blanchard, 1968; Blanchard and Boswell, 1925; Velasco et al., 2013). *Indigenous limonite* is defined as "limonite" precipitated from iron-bearing solutions within the cavity formerly occupied by the sulfides from which the iron is derived. Siliceous-sponge limonite is indicative of the previous massive sulfide mineralization (e.g. Andrew, 1980; Blanchard, 1968) usually preserved in box-work or cellular textures. In contrast, *transported limonite* represents limonitic assemblages moved a short distance (a few centimeters) from the former sulfide (Blanchard, 1968). Alpers and Brimhall (1989) use the term *transported limonite* to refer to those oxidized facies where iron has clearly moved from its original source and was precipitated in non-sulfide sites, generally in fractures or as a pervasive stain (*i.e.* exotic limonite described by Blanchard, 1968). The term *exotic limonite* was used by Blanchard (1968) to describe when Fe is transported outside the confines of the orebody, commonly up to a hundred meters away. Boyle (2003) suggested the concept of chemical reworking to determine the indigenous or transported character of a gossan.

Both indigenous and transported textural features are widely found at Cerro de Maimón gossan. Several textures characteristic of transported gossan are easily observed along the profile. Indeed, breccia and rubbly lithofacies (Fig. 3E), oxides precipitated along fractures outside the confines of the orebody (Fig. 3I), idiomorphic barite crystals over limonitic assemblages has been suggested by many authors as characteristics of transported gossans (e.g. Alpers and Brimhall, 1989; Blanchard, 1968; Boyle, 2003). On the contrary, wide areas of cellular oxides replacing previous sulfides as well as relicts of sulfides among cellular goethitic lithofacies (Fig. 5E) suggest an indigenous character.

Although both characteristics are recognizable, the Cerro de Maimón gossan cannot be considered as transported since the primary and supergene copper sulfides are beneath the oxide body (Fig. 2B). The reason of the coexistence of both types is possibly due to i) the schistose character of the host formation, ii) the steep position of the mineralized lenses and iii) the seasonal intense rainfall typical of tropical climates. The tectonized condition of the deposit could enable the percolation of waters through the schistosity and late fissures, enhancing dissolution-precipitation processes along fractures and sheared zones. This phenomenon leads to subsequent collapse and hence transport of the gossan along fractures.

7.2. Genetic evolution of the profile

The genetic evolution of the orebody is controlled by the existing fracture system. Alvaro and Velasco (2002) and Capitán et al. (2003) suggested that gossan evolution can be divided into three main stages: i) the oxidative dissolution of the sulfides, ii) the evolution of the former oxyhydroxides and iii) the mechanical reworking of the previously formed oxides. These stages in evolution are applicable to the Cerro de Maimón gossan as follow.

As result of the weathering of the sulfide orebody, the oxidative dissolution of the sulfides takes place at low pH conditions preserving the original sulfide box-work (if pH > 3) or leaching along with transport of Fe-rich solutions (if pH < 3) (Blain and Andrew, 1977; Sillitoe and Clark, 1969). Colloform textures are formed once these leached Fe-rich waters reach near-neutral pH conditions. This process implies an important loss of volume and mass that would explain the abundance of botryoidal textures in the upper part of the profile together with cavernous layers

Please cite this article as: Andreu, E., et al., Weathering profile of the Cerro de Maimón VMS deposit (Dominican Republic): textures, mineralogy, gossan evolution and mobility of..., Ore Geol. Rev. (2014), http://dx.doi.org/10.1016/j.oregeorev.2014.09.015

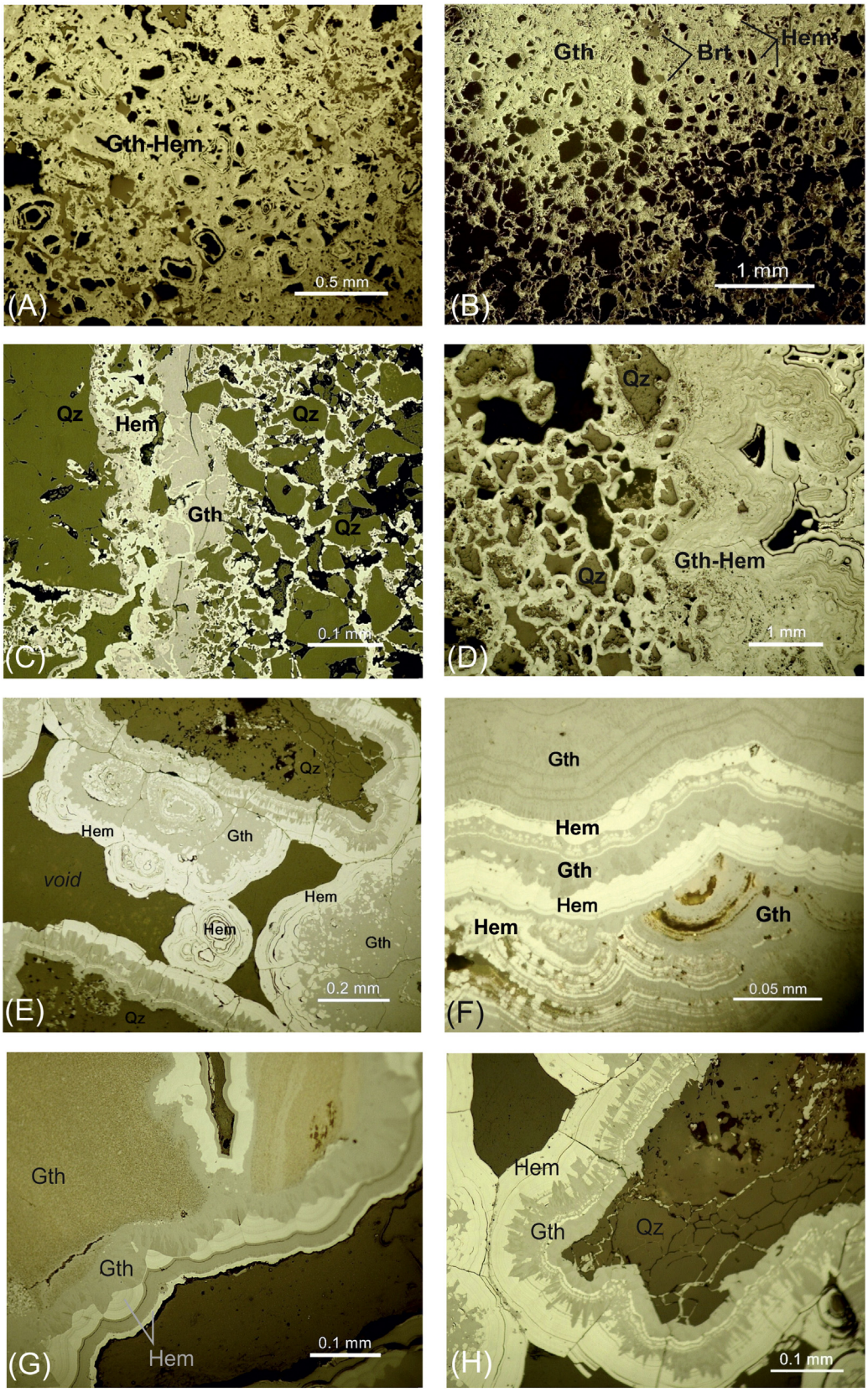

showing geopetal and stalactite morphologies related to/associated to rock debility planes such as schistosity.

The evolution of the previously formed oxides and hydroxides (also known as ageing or maturation) starts when most of the sulfides above the water table are oxidized. At this point, the acidity generation process is interrupted and ground waters evolve to less acidic conditions. The initially formed iron oxyhydroxides are more likely to be poorly crystalline (e.g. ferrihydrite), as they may contain excessive water in their

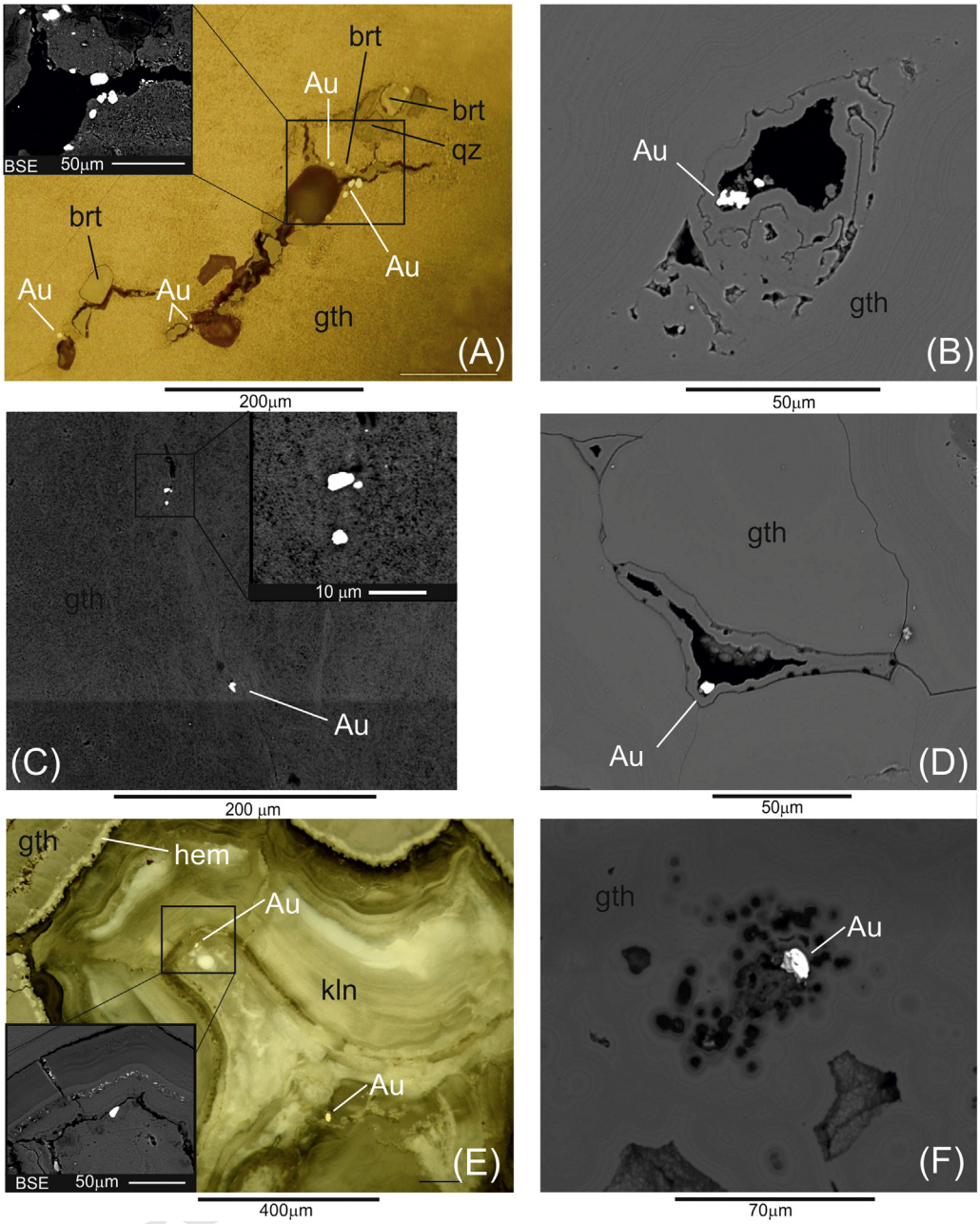

Fig. 6. Reflected light (A and E) and SEM-BSE images of some of the identified gold grains. A: Fine grained goethite (mustard-colored) showing a cluster of high purity gold grains in a shrinkage crack. B: Reinform gold grain located inside a void left among colloform aggregates. C: Fine grained goethite showing several sub-rounded gold grains. D: Rounded gold grain inside a void left among colloform aggregates. E: Gold grains observed within layers of kaolinite suggesting a late transport of gold grains dragged by clayey minerals during reworking stages. F: Gold grain infilling spongy pores left among layers of colloform oxides. Abbreviations: Qz: quartz; Gth: goethite; Hem: hematite; Brt: barite.

structure (Taylor and Thornber, 1992). Fine grained goethitic layers are considered to be amorphous iron hydroxides such as ferrihydrite transformed to goethite by dehydration and hematite (Alpers and Brimhall, 1989; Schwertmann and Murad, 1983). These layers represent the latest episodes of gossan formation and may be linked to old water table levels (Alpers and Brimhall, 1989; Blain and Andrew, 1977). Hematite is likely formed by a dehydration or aging process after goethite or ferrihydrite (Alpers and Brimhall, 1989; Capitán et al., 2003). The studied polished samples systematically showed an outer rim of hematite (Fig. 5A) and examples of fine grained goethite transforming to crystalline goethite (Fig. 5G and H), both indicatives of gossan ageing.

Fig. 5. Reflected light photomicrographs of the most representative textures identified along the Cerro de Maimón weathered profile. A: Cellular textures preserving the shape of the former sulfides in boxwork and ladderwork microtextures. Barite and silica are left as residues among oxides. B: Cellular textures showing a progressive variation in the degree of oxide cementation. These variations (also observed in rubbly textures) suggest oxide precipitation fronts, controlling collapse and breccia formation processes. Barite and silica are left as residues among oxides. C: Microbreccia texture showing several silica fragments cemented by goethite and hematite. D: Microbreccia acting as a substrate for the development of botryoidal aggregates showing the variability of facies at the millimeter scale. E: Massive-

Please cite this article as: Andreu, E., et al., Weathering profile of the Cerro de Maimón VMS deposit (Dominican Republic): textures, mineralogy, gossan evolution and mobility of..., Ore Geol. Rev. (2014), http://dx.doi.org/10.1016/j.oregeorev.2014.09.015

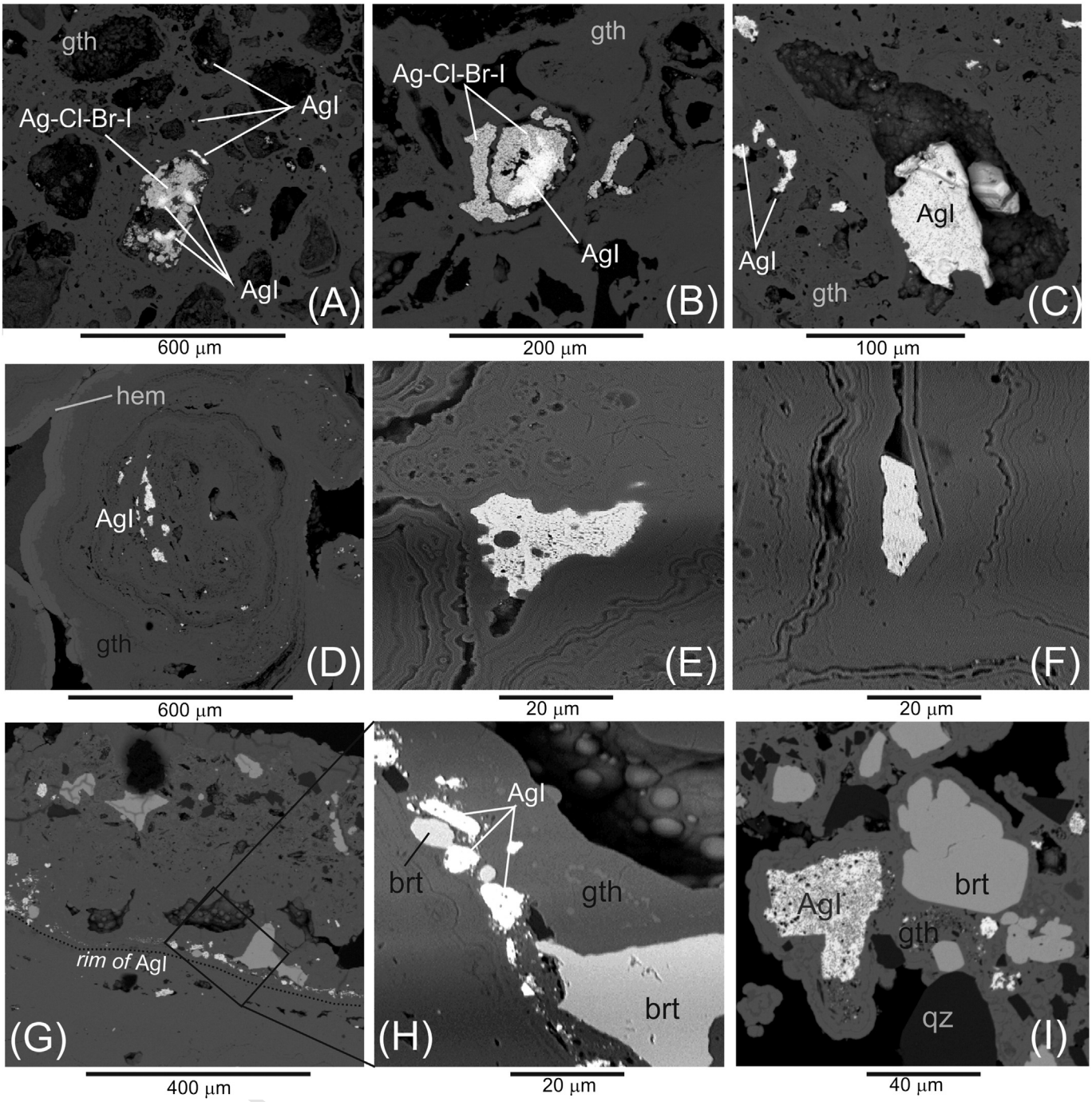

Fig. 7. SEM-EDS images of silver halides observed in the Cerro de Maimón gossan. Note the spongy texture of the halides. A and B: Zoned "embolite" grains showing an inner core of AgI and Cl-Br-rich boundaries. Note the tiny sparks of AgI widespread in pores. C: Euhedral AgI crystals inside a void of massive-botryoidal lithofacies suggesting precipitation of AgI after the formation of the oxides. D; Goethitic colloform aggregate showing multiple grains of AgI filling voids between successive botryoidal layers. E and F: Detail of AgI grains filling voids of colloform aggregates suggesting late episodes of AgI precipitation. G: Rim of AgI and barite fragments cemented in a massive-rubbly lithofacies. H: Detail of picture G, suggesting late stages of gossan reworking probably due to dissolution-collapse episodes. I: Spongy fragment of AgI (similar to those observed in pictures E and F) cemented by oxides together with residual barite and quartz. Abbreviations: Qz: quartz; Gth: goethite; Brt: barite.

The last stage, consisting of a physical reworking of the previously formed morphologies, is produced by collapse of the oxide orebody. Indeed, the presence of iodargyrite and barite fragments (both highly insoluble) cemented by botryoidal aggregates suggests late events of oxide-dissolution, transport and precipitation of Fe-rich solutions dragging and bearing fragments of insoluble minerals, co-eval with late repetitions of the firsts stages processes (Fig. 7G, H and I).

7.3. Supergene enrichment mechanisms. Mobility of gold and silver in the gossan profile

The weathering profile shows supergene enrichment in gold and silver. The vertical distribution of the studied gold-bearing samples does not follow a clear trend since discrete gold grains are found at different depths. Indeed, the Au-richest layers coincide with thin, yellow-mustard colored and humid levels of poorly crystalline goethite. These

Table 1
Summary of representative analyses of Au- and Ag- bearing minerals from Cerro de Maimón gossan analyzed by EMP.

Mineral	Native gold	Native gold	Iodargyrite	Embolite	Embolite
Sample	CM-190A-2a	CM-190A-3	cer1b	cer1b	cer1a
Fe W%	d.l.	d.l.	2.82	4.25	0.74
Ni W%	d.l.	d.l.	-	-	-
Cu W%	d.l.	d.l.	d.l.	0.22	d.l.
Zn W%	d.l.	d.l.	-	-	-
As W%	d.l.	d.l.	d.l.	d.l.	0.36
Ag W%	d.l.	d.l.	54.49	78.37	74.45
Sb W%	0.15	0.14	-	-	-
Au W%	98.38	98.35	-	d.l.	-
Hg W%	-	-	-	d.l.	-
Pb W%	d.l.	d.l.	-	-	-
I W%	-	-	42.48	0.96	4.92
Br W%	-	-	0.12	11.88	13.08
Cl W%	-	-	0.07	3.08	5.10
Sum W%	**98.53**	**98.49**	**99.98**	**98.76**	**98.65**
Fe A%	-	-	5.65	7.45	1.31
Ni A%	-	-	-	-	-
Cu A%	-	-	-	0.34	-
Zn A%	-	-	-	-	-
As A%	-	-	-	-	0.48
Ag A%	-	-	56.55	71.11	68.41
Sb A%	0.25	0.23	-	-	-
Au A%	99.75	99.77	-	-	-
Hg A%	-	-	-	-	-
Pb A%	-	-	-	-	-
I A%	-	-	37.48	0.74	3.84
Br A%	-	-	0.17	14.56	16.23
Cl A%	-	-	0.15	5.80	9.72

layers can be observed at different depths, but they are thicker at depth, just above supergene sulfides. Ag, as reported in Section 6, mainly occur forming iodargyrite (AgI) and Cl-Br-I Ag-halides.

Gold enrichment ratio in the Cerro de Maimón gossan, calculated as *oxide ore grade/sulfide ore grade*, is 1.4 (in clayey goethitic layers the ratio increases up to 33). However, silver enrichment ratio is only 0.5 (i.e. loss of Ag in the oxide ore). The abundance of Ag-halides together with the state of the high fineness of gold (99.4 at.% Au) and the antagonistic gold and silver enrichment ratio in Cerro de Maimón gossan suggest both an efficient Au-enrichment/Ag-leaching process during gossan formation and a large availability of halide ligands during weathering.

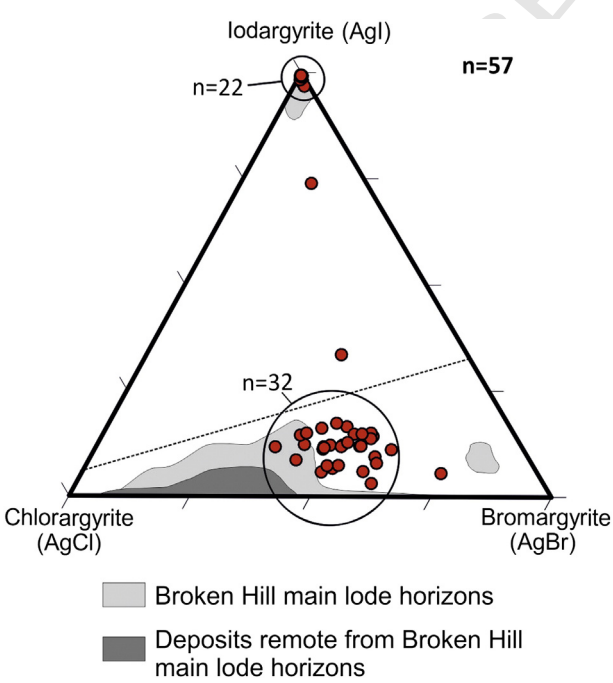

Fig. 8. Normalized microprobe results of selected Ag-halides grains plotted in a triangular diagram, showing the Cl-Br-I end-members (chlorargyrite, bromargyrite and iodargyrite respectively). Represented fields of Ag-halides from Broken Hill were drawn from data by Gillard et al. (1997). See text for description.

Supergene enrichment in gold (and silver) in the weathering profile can be due to either chemical or physical processes (residual, detrital gold) or to a combination of both. Mechanisms producing the chemical leaching and transport of gold and silver in weathering environments strongly depend on the availability of anionic ligands and/or on the redox conditions of the aqueous system (Freyssinet et al., 2005). Complexing agents include halides (mainly Cl, Br and I), organic complexes and colloids, and sulfur-bearing species (Bowell et al., 1993; Colin et al., 1993; Freyssinet et al., 2005; Mann, 1984; Stoffregen, 1986; Webster and Mann, 1984).

Both Au and Ag form aqueous halide complexes and, in the case of Ag, also solid phases. However, Ag-halide aqueous complexes are reported to be stronger than that of Au-halides; in the same way, aqueous Au- and Ag-iodide complexes are stronger than bromide and chloride Au- and Ag-complexes (Gammons and Yu, 1997; Gray et al., 1992).

Detailed examination of the Eh-pH predominance diagrams for the Au and Ag Cl-Br-I-H_2O systems (Fig. 9A and B) reveals the predominance of Au-I and Ag-I species and solid phases over other Ag- and Au-Cl and Br complexes under the Eh-pH conditions reported for tropical areas (Bertolo et al., 2006; Bowell et al., 1993). For this reason, AgI(aq) is the predominant aqueous species and iodargyrite (AgI) predominates over chloride or bromide Ag solid phases (that would be stable only if iodide further oxidized to iodate) (Fig. 9A). The preferential formation of iodargyrite over bromargyrite and chlorargyrite can be explained by its lower solubility (Gammons and Yu, 1997; Golebiowska et al., 2010) and suggest an external contribution of iodine able to decrease the high Cl/(F + Br + I) ratio observed in natural waters, that frequently enhances the formation of chlorargyrite (Boyle, 1997; Gammons and Yu, 1997). The source for this iodine is discussed below.

Given its low solubility, crystalline Au widely predominates against any of the other Au species (Fig. 9B). The close association of gold and goethite observed in the gossan can be explained by the precipitation of Au(s) after the reduction of aqueous Au^+ by the oxidation of the aqueous Fe(II) produced by the weathering of the former sulfides (Freyssinet et al., 2005; Gray et al., 1992; Mann, 1984). Then, in those conditions in which gold precipitates as Au(s), silver remains in solution (Mann, 1984) and is transported away from the site of gold deposition enhancing the purity of gold grains. The preferential adsorption of Au onto Fe-oxyhydroxide surfaces (e.g. Cohen and Waite, 2004; Karasyova et al., 1998; Ran et al., 2002) explains the tight relation between Au and amorphous Fe-oxyhydroxide assemblages.

Smith and Hunt (1985) and Nahon et al. (1992) revealed that the presence of organic compounds such as cyanide or humic and fulvic acids released by plants or microorganisms can play a remarkable role in gold mobility. Biogenic morphologies of Au grains have been recognized as evidences of biomineralization of precious metals under weathering conditions (Lengke and Southam, 2007; Reith et al., 2006; Watterson, 1991). At Cerro de Maimón, reinformed high purity Au-grains have been identified inside pores within botryoidal goethite aggregates (Fig. 6B) so that a biogenic mineralization in addition to Fe^{2+} oxidation and the reduction of Au halides cannot be ruled out.

7.4. Sources of iodine

According to Gammons and Yu (1997), the occurrence of AgI within a gossan suggests a renewable contribution of iodine to the system during the supergene enrichment and the gossan formation period. Reich

Please cite this article as: Andreu, E., et al., Weathering profile of the Cerro de Maimón VMS deposit (Dominican Republic): textures, mineralogy, gossan evolution and mobility of..., Ore Geol. Rev. (2014), http://dx.doi.org/10.1016/j.oregeorev.2014.09.015

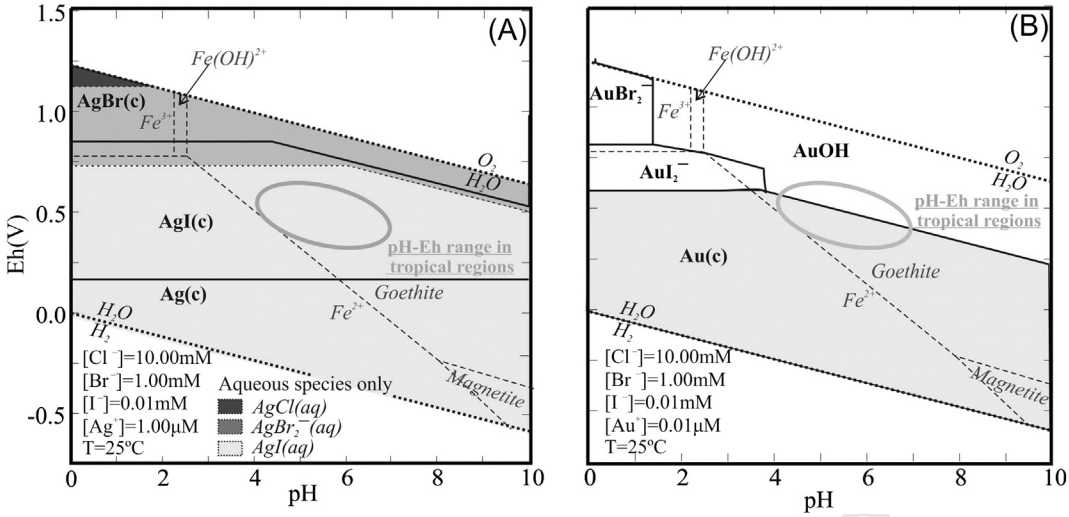

Fig. 9. Predominance Eh-pH diagrams of the Ag/Au-Cl-Br-I-H_2O and Fe systems. Diagrams were performed using "MEDUSA" code and "HYDRA" database (Puigdomènech, 2010). Concentrations used are shown in the diagrams. Ellipse shows the range of Eh and pH values typical of tropical regions (Bertolo et al., 2006; Bowles et al., 1993). A: Ag-Cl-Br-I-H_2O system showing that he widest predominance area corresponds to AgI, even when I- concentration is 103 times lower than Cl-. Shadowed areas correspond to the stability areas of aqueous species suggesting that $AgI_{(aq)}$ would be the predominant specie for Ag-mobility. B: Au-Cl-Br-I-H_2O system showing that crystalline gold is the predominant phase under normal groundwater conditions. However at higher I- activities, Au would be preferentially complexed and transported as AuI_2- even at high Cl- and Br- activities.

et al. (2009) reached a similar conclusion at the Mantos de la Luna Cu deposit (Chile) where the occurrence of inclusions of iodargyrite in supergene chalcocite involved iodine-rich waters during supergene enrichment.

Iodine concentration in freshwater and seawater is very low (<100 ppb) (Gammons and Yu, 1997; Hem, 1985; Moran et al., 1999; Reich et al., 2009) but it appears to be higher in deep brines and pore waters, where concentrations may exceed 100 ppm (Muramatsu et al., 2001; Reich et al., 2009).

The Earth's crust is also iodine-poor (Reich et al., 2009), with low ppb values in igneous and metamorphic rocks. Peatlands are the largest terrestrial iodine pool (Keppler et al., 2004). As summarized in Reich et al. (2009, 2013) and Osborn et al. (2012), iodine is mainly accumulated in marine sediments, where concentrations are more than 100 times higher than in seawater (Moran et al., 1995, 1999; Muramatsu and Wedepohl, 1998; Muramatsu et al., 2001, 2004). Scholz et al. (2010), Cabral et al. (2011) and references therein explain that this enrichment in marine sediments is due to the high biophile character of iodine that enhances the assimilation of iodine by phytoplankton in surface waters. Iodine is then accumulated on the sediment surface when organic matter sinks. During early diagenesis, part of this iodine associated to organic matter is released to pore water and is again assimilated by phytoplankton and recycled in the surface sediments (Harvey, 1980; Kennedy and Elderfield, 1987a,b; Price and Calvert, 1973). Another portion is buried, as observed in continental margins with stored organic carbon and associated compounds (Fehn et al., 2007a). Subsequently, microbial or thermal decomposition of this organic matter can produce high concentrations of iodine in deep interstitial fluids. Under very reducing conditions, iodide is the stable phase of iodine in pore water (see Fig. 9A). Given its large ionic radius, I is a minor component of minerals and tends to remain within the aqueous phase (Fehn et al., 2007b; Osborn et al., 2012; Scholz et al., 2010).

There is still discussion in the literature concerning the different iodine sources that may account for the increase of iodine concentration and the precipitation of iodargyrite in supergene and gossan environments. Isotopic measurements to calculate $^{129}I/I$ together with $^{87}Sr/^{86}Sr$ ratios have been used to discern the origin of iodine rich waters (Daraoui et al., 2012; Fabryka-Martin et al., 1985; Osborn et al., 2012; Reich et al., 2013; Scholz et al., 2010). $^{129}I/I$ ratio is a useful tracer in reconstructing deep regional paleohydrological flow systems because of its relatively long half-life ($t_{1/2} = 15.7$ Ma) and mobility in an aqueous system (Osborn et al., 2012). Unfortunately, there are not any available isotope measurements in the case of Cerro de Maimón VMS; different options for the origin of its halides are proposed.

A possible source of the iodine in Cerro de Maimón could be deep groundwaters flowing through the deposit.

Boyle (1997) and references therein pointed out the close proximity of Ag-halide deposits and salt lake formations in Nevada, New Mexico and Utah. They concluded that as these areas were covered by large bodies of water during the Tertiary and gradually dried up, the concentration of halides in pore water would have increased providing the iodine for the formation of iodargyrite. Boyle (1997) considered that the saline water originated by evaporation of a lake or sea located close to the deposit and was thus the main source of iodine. It has also been suggested that seismic pumping of highly saline iodine-rich deep formation waters and/or fore-arc fluids along faults and fractures (Cameron et al., 2002, 2007; Palacios et al., 2005) is the way the iodine reaches the deposit. As an example, Reich et al. (2009) proposed that the origin of iodine in the Cu deposit of Mantos de Luna (Chile) was a saline iodine-rich deep formation water and/or a fore-arc fluid that was forced to the surface by seismic pumping through fractures; after leaching the Cu sulfides this led to the formation of iodargyrite under near-neutral to acidic reducing conditions. Golebiowska et al. (2010) proposed either the evaporation of a former sea or salt lake or the infiltration of saline iodine-rich deep formation water as the sources to explain the presence of iodargyrite in the Zalas deposit (Poland) but that this is still a theme under debate. The use of ^{129}I measurements allowed Reich et al. (2013) to conclude that the iodine responsible of the formation of marshite (CuI) in Chuquicamata deposit (Chile) is derived from a reservoir of marine origin of lower Jurassic to mid Cretaceous age, rather than from a meteoric/atmospheric source.

Another possible source of halides, as pointed out by some authors, is the Caribbean Sea or the Atlantic or Pacific oceans, via a marine influence on rainfall (Mann, 1984) or even oceanic water lifted up and transported by the seasonal hurricanes. Whiterhead (1919) suggested that the source of halides for the Ag-halide deposits of Chañarcillo (Chile) were sea-salt particles from the Pacific Ocean that would have traveled with the wind, deposited on the surface, concentrated by evaporation and moved down into the supergene zone during the precipitation periods. In fact, African dust supplies critical nutrients to the

Please cite this article as: Andreu, E., et al., Weathering profile of the Cerro de Maimón VMS deposit (Dominican Republic): textures, mineralogy, gossan evolution and mobility of..., Ore Geol. Rev. (2014), http://dx.doi.org/10.1016/j.oregeorev.2014.09.015

Amazon basin and therefore it could play a similar role in the Caribbean and the Bahamas zones (Swap et al., 1992). Prospero and Mayol-Bracero (in press) showed that Saharan dust accounts for over half of the global dust emissions throughout the Caribbean.

In addition, in their genetic model explaining the presence of iodargyrite in the Rubtsovskoe VMS-base metal deposit of Altai (Russia), Pekov et al. (2011) proposed a source of iodine related to sea-floor fumaroles accompanying ore formation. Iodide would have been adsorbed onto the clay minerals of the argillic alteration zone of the wall rock and oxidized to iodate by the sulfuric acid generated during the first stages of sulfide ore oxidation. Once released into solution, iodate would have been reduced to iodide and precipitated as AgI or CuI.

During the supergene enrichment and formation of the gossan in Cerro de Maimón, the deposit was covered with a soil layer with a thickness of 2.5–3 m. Keppler et al. (2004) reported that organic-rich soils present a high capacity to retain and store iodine through the formation of organoiodine compounds. The organic matter content in tropical soils is not negligible (Six et al., 2002) and thus, Caribbean soil can be considerably rich in iodine. Intense soil lixiviation by meteoric waters and/or of reduction of IO_3^- by oxidation of the structural Fe(II) in some clays (Hu et al., 2005) could have released I^- to porewater and precipitated as AgI.

Considering the geological, mineralogical and geochemical data available for the Cerro de Maimón deposit, the choice of a unique source for iodine is not straightforward and discussion remains open.

7.5. Is iodargyrite a climate indicator?

Many authors suggest that the occurrence of Ag-halide minerals, and especially that of iodargyrite, is only given in oxidized sulfide zones formed in arid and semi-arid environments (Boyle, 1994, 1997; Burgess, 1911; Penrose, 1894). This conclusion arose from an investigation of the relative proportions of halide minerals in different metallogenic provinces (Boyle, 1997). Since then, and considering some other climate indicators, the occurrence of iodargyrite has been used to suggest and/or confirm the existence of arid or semi-arid climates, such as desert areas of Atacama, Chile (Reich et al., 2009), Broken Hill, Australia (Millsteed, 1998), Mohave Desert in California, Nevada and central Kazakhstan desert (Boyle, 1997), Zalas in Poland (Golebiowska et al., 2010) and Iberian Pyrite Belt (Velasco et al., 2013) during the AgI formation.

Taking into account the global evolution of temperature, it is known that on a world scale, the late Eocene to middle Oligocene was characterized by some of the warmest temperatures observed (Shacketon, 1978). Although the global warming in Oligocene time might also affected the Caribbean zone, since the formation of the primitive island arc during the Early Cretaceous to the present day, the Caribbean has been located within tropical latitudes. Thus, the Caribbean surface geology has evolved under tropical conditions with seasonal rainfall and high moisture. The northern part of the Cordillera Central, where Cerro de Maimón is located, was formed during the Miocene (Mann et al., 1991), and hence the surface geology over the deposit developed later than this warmest period. Moreover, in the region there is no evidence of typical formations of arid environments such as evaporites or red-clays facies.

All these considerations indicate that the formation of AgI in the Cerro de Maimón gossan did not take place under arid nor semi-arid climate conditions pointing out that the occurrence of iodargyrite does not necessarily imply arid environments but the presence of saline-halide rich groundwater in oxide deposits.

7.6. Metallurgical implications

At Cerro de Maimón processing plant, the oxide ore is processed via grinding in a ball mill to 80 % passing 105 μm followed by conventional agitated cyanide leaching, counter current decantation thickening (pH 11) and Merrill-Crowe Au-Ag precipitation at a projected rate of 700 tpd. The main problems on the oxide ore treatment are concerned with a lower than expected silver recuperation and a higher than expected copper contents in the produced *doré* bars.

Gold in the oxide ore is present as free native grains as described above. Thus, the recuperation of gold does not represent a problem. In contrast, silver is present as iodargyrite and other Ag-halides, which may be easily leached by cyanide. However, remarkable quantities of silver could be present as a diluted solid solution within the goethite-rich assemblage as happens to jarosite in other deposits (230 ppm of invisible Ag on average, Roca et al., 1999) or secondary sulfides (up to 2000 ppm of invisible Ag, Kojima et al., 2003; Reich et al., 2008). If an important part of the silver occurs as a diluted solid solution within the limonitic assemblage, conventional cyanidation will not leach it and the recoveries will keep low.

In the case of the higher than expected copper content in the *doré*, the source of the problem may be the Cu^{2+}-rich nature of the interstitial ground waters, especially in the base of the oxidized zone. Another possibility might be a slight contamination by Cu-rich sulfides in the crushing plant (oxide ore and sulfide ore are crushed in the same circuit). Cu-bearing sulfides and Cu^{2+}-species are preferentially complexed by CN^- enhancing the consumption and oxidation of cyanide (Zhang et al., 1997).

The same problem has been faced by similar mining projects, for example, the gossans of Rio Tinto district (Roca et al., 1999; Viñals et al., 1995, 2003). The paragenesis of those gossans basically consists of goethite, hematite and solid solutions of beudantite-plumbojarosite-potassium jarosite. Silver occurs as halide, sulfide, Hg-Ag sulfo-halide and as a low-grade solid solution of argentojarosite in jarosite-beudantite phases (Roca et al., 1999). In these cases the solid solutions of beudantite-plumbojarosite-potassium jarosite were not decomposed during conventional cyanidation. Viñals et al. (1995, 2003) and Roca et al. (1999) studied the extraction of invisible Ag in oxide ores through autoclave alkaline decomposition and cyanidation.

In the case of Cerro de Maimón ore, further studies are necessary to test the feasibility of such a process. Those studies should take into account that the main difference from the oxide ores of Rio Tinto is the lack of jarosite-beudandite assemblages and the fact that silver might be hosted in goethite. The techniques recommended to be used should consist in a sequential acid leaching coupled with XRD analysis to determine if iodargyrite (and embolite) is the only Ag-bearing mineral.

8. Conclusions

The results of this study have led to the following statements/conclusions:

1) The oxide paragenesis is broadly composed of goethite, hematite, quartz and barite. Botryoidal, cellular and brecciated textures can be distinguished. Botryoidal and brecciated textures dominate in the upper parts of the oxide body, whereas cellular textures are more common in the intermediate and lower parts of the deposit. However, the weathering profile is very heterogeneous.
2) The gossan profile shows evidence of being both transported and indigenous. The steep position of the oxide lens, as well as the steep dip of the remnant schistosity and the intense rainfall and moisture of the tropical climate played an important role. Waters percolate in more permeable zones developing brecciated (after collapse) and botryoidal textures.
3) The lack of jarosite suggests that pH conditions were not extremely acidic since the pluviosity of the tropical climate probably plays a dilution/buffering effect on the acidification process.
4) Gold grains in the oxide paragenesis are extremely pure (99 % Au) suggesting that a chemical purification took place. Gold grains occur in pores among botryoidal goethite aggregates and/or

Please cite this article as: Andreu, E., et al., Weathering profile of the Cerro de Maimón VMS deposit (Dominican Republic): textures, mineralogy, gossan evolution and mobility of..., Ore Geol. Rev. (2014), http://dx.doi.org/10.1016/j.oregeorev.2014.09.015

shrinkage fractures in fine goethite layers. The location and purity of gold suggests an *in situ* precipitation.

5) Silver occurs mainly as iodargyrite (AgI), and minor AgBr, AgI, in botryoidal aggregates. The shape of the grains, systematically less than 20 μm, adapts to the shape of the pore. The morphology and location of iodargyrite grains also indicate an *in situ* precipitation.
6) Halides are effective Au-Ag leaching agents. In the presence of halides, gold and silver can be transported in a wide range of pH-Eh conditions, especially if iodine is present. Silver is leached more rapidly and over a broader range of pH-Eh conditions. It is also preferentially transported as iodine-complexes than other halides.
7) Since Cerro de Maimón fully developed under tropical conditions, the presence of Ag-halides cannot be considered intrinsic of arid environments as commonly stated. These minerals are rather indicators of the presence of saline-halide rich groundwater in oxide deposits.
8) The lower than expected silver recovery in the oxide treatment plant could be due to undetermined amounts of silver present as a diluted solid solution within the limonitic assemblage. In that case, classical leaching methods are not efficient as has been described in Ag-bearing jarositic assemblages.

Acknowledgments

This research has been financially supported by the Spanish project CGL2012-36263, the Catalan project SGR 2009-444 and two FPU Ph.D. grants to L.T. and C.V.deB. by the Ministerio de Economía y Competitividad of the Spanish Government. The help and hospitality extended by the staff at Cerro Mamón mine are also gratefully acknowledged, as well as the technical support in EMP sessions by Dr. X. Llovet and Dr. A. Viñals (R.I.P.) for their useful comments and suggestions on metallurgical treatment of Au-Ag rich oxide/gossan. The comments and corrections of the two anonymous reviewers clearly improved the quality of the manuscript.

References

Alpers, C.N., Brimhall, G.H., 1989. Paleohydrologic evolution and geochemical dynamics of cumulative supergene metal enrichment at La Escondida, Atacama Desert, Northern Chile. Econ. Geol. 84, 229–255.
Alvaro, A., Velasco, F., 2002. Etapas de alteración supergenica en la formación del gossan de San Miguel (Faja Piritica Iberica). Bol. Soc. Esp. Mineral. 25A, 3–4.
Andreu, E., Proenza, J.A., Tauler, E., Chavez, C., Espaillat, J., 2010. Gold and Iodargyrite in the Gossan of Cerro de Maimón Deposit (Central Dominican Republic). Macla 13, 41–42.
Andrew, R.L., 1980. Supergene alteration and gossan textures of base-metals ores in southern Africa. Miner. Sci. Eng. 12, 193–215.
Astacio, V.A., Lewis, J.F., Campbell, A., Espaillat, J., 2000. Oxygen isotope and alteration geochemistry of the Cerro de Maimón deposit, Dominican Republic. In: Jackson, T. (Ed.), Caribbean geology in the new millenium, transactions 15th Caribbean geological conference, Kingston, Jamaica.
Belogub, E.V., Novoselov, K.A., Yakovleva, V.A., Spiro, B., 2008. Supergene sulfides and related minerals in the supergene profiles of VHMS deposits from the South Urals. Ore Geol. Rev. 33, 239–254.
Bertolo, R., Hirata, R., Sracek, O., 2006. Geochemistry and geochemical modeling of unsaturated zone in a tropical region in Urania, Sao Paulo state, Brazil. J. Hydrol. 329, 49–62.
Blain, C.F., Andrew, R.L., 1977. Sulfide weathering and the evaluation of gossans in mineral exploration. Miner. Sci. Eng. 9, 119–149.
Blanchard, R., 1968. Interpretation of leached outcrops. 66. Nevada Bureau of Mines Bulletin, (169 pp.).
Blanchard, R., Boswell, P.F., 1925. Notes on the oxidation products derived from chalcopyrite. Econ. Geol. 20, 613–638.
Bowell, R.J., Foster, R.P., Gize, A.P., 1993. The mobility of gold in tropical rain forest soils. Econ. Geol. 88, 999–1016.
Bowin, C.O., 1966. Geology of the central Dominican Republic. Geol. Soc. Am. Mem. 98, 11–84.
Boyle, D.R., 1994. Oxidation of massive sulfide deposits in the Bathurst Mining Camp: natural analogues for acid drainage in temperate climates. In: Alpers, C.N., Bowles, D.W. (Eds.), Environmental geochemistry of sulfide oxidation. American Chemical Society, pp. 535–550.
Boyle, D.R., 1997. Iodargyrite as an indicator of arid climatic conditions and its association with gold-bearing glacial tills of the Chibougamau-Chapais area, Quebec. Can. Mineral. 35, 23–34.
Boyle, D.R., 2003. Preglacial weathering of massive sulfide deposits in the Bathurst mining camp: Economic geology, geochemistry, and exploration applications. In: Goodfellow, W.D., McCutcheon, S.R., Peter, J.M. (Eds.), Massive sulfide deposits of the Bathurst mining camp, New Brunswick, and northern Maine. Econ. Geol. Monograph 11, pp. 689–721.
Brownell, G.M., Kinkel, A.R. Jr, 1935. The Flin Flon mine: geology and parargenesis of the ore deposits. Canadian Inst. and Met. Tr. 28 (Bull no. 279), pp. 261–286.
Bruce, J.L., 1948. Cyprus mines copper again. Min. Tech. A.I.M.E., T.P. 245.
Burgess, J.A., 1911. The halogen salts of silver associated minerals at Tonopah, Nevada. Econ. Geol. 6, 13-12. Q7
Cabral, A.R., Radtke, M., Munnik, F., Lehmann, B., Reinholz, U., Riesemeier, H., Tupinambá, M., Kwitko-Ribeiro, R., 2011. Iodine in alluvial platinum-palladium nuggets: Evidence for biogenic precios-metal fixation. Chem. Geol. 281, 152-132. Q8
Cameron, E.M., Leybourne, M.I., Kelley, D.L., 2002. Exploring for deeply covered mineral deposits: Formation of geochemical anomalies in northern Chile by earthquake-induced surface flooding of mineralized groundwaters. Geology 30, 1007–1010.
Cameron, E.M., Leybourne, M.I., Palacios, C., 2007. Atacamite in the oxide zone of copper deposits in northern Chile: involvement of deep formation waters? Miner. Deposita 42, 205–218.
Capitán, A., Nieto, J.M., Sáez, R., Almodovar, G.R., 2003. Caracterización textural y mineralógica del gossan del Filón Sur (Tharsis, Huelva). Bol. Soc. Esp. Mineral. 26, 45–58.
Cohen, D.R., Waite, T.D., 2004. Interaction of aqueous Au species with goethite, smectite and kaolinite. Geochem. Explor. Environ. Anal. 4, 279–287.
Colin, F., Vieillard, P., Ambrosi, J.P., 1993. Quantitative approach to physical and chemical gold mobility in equatorial rainforest lateritic environment. Earth Planet. Sci. Lett. 114, 269–285.
Colomer, J.M., Andreu, E., Torró, L., Proenza, J.A., Melgarejo, J.A., Chavez, C., del Carpio, R., Espaillat, J., Lewis, J.F., 2013. Mineralogy, textures and new sulphur isotope data of the Cerro de Maimón VMS deposit ores, Dominican Republic. Mineral deposit research for a high-tech world. Proceedings of the 12th Biennial SGA Meeting. 2. ISBN: 978-91-7403-207-9, pp. 518–521.
Daraoui, A., Michel, D., Gorny, M., Jakob, D., Sachse, R., Synal, H.A., Alfimov, V., 2012. Iodine-129, Iodine-127 and Caesium-137 in the environment: soils from Germany and Chile. J. Environ. Radioact. 112, 8–22.
Draper, G., Gutiérrez, G., Lewis, J.F., 1996. Thrust emplacement of the Hispaniola peridotite belt: orogenic expression of the mid Cretaceous Caribbean arc polarity reversal? Geology 24, 1143–1146.
Escuder-Viruete, J., Contreras, F., Joubert, M., Urien, P., Stein, G., Weis, D., Pérez-Estaún, A., 2007a. Tectónica y geoquímica de la Formación Amina: registro del arco isla Caribeño primitivo en la Cordillera Central, República Dominicana. Bol. Geol. Min. 118, 221–242.
Escuder-Viruete, J., Contreras, F., Stein, G., Urien, P., Joubert, M., Pérez-Estaún, A., Friedman, R., Ullrich, T., 2007b. Magmatic relationships between adakites, magnesian andesites and Nb-enriched basalt-andesites from Hispaniola: Record of a major change in the Caribbean island arc magma sources. Lithos 99, 151–177.
Escuder-Viruete, J., Pérez-Estaún, A., Weis, D., Friedman, R., 2009. Geochemical characteristics of the Río Verde Complex, Central Hispaniola: Implications for the paleotectonic reconstruction of the Lower Cretaceous Caribbean island-arc. Lithos 114, 168–185.
Fabryka-Martin, J., Bentley, H., Elmore, D., Airey, P.L., 1985. Natural I-129 as an environmental tracer. Geochim. Cosmochim. Acta 49, 337–347.
Fehn, U., Moran, J.E., Snyder, G.T., Muramatsu, Y., 2007a. The initial I-129/I ratio and the presence of "old" iodine in continental margins. Nucl. Inst. Methods Phys. Res. B 259, 496–502.
Fehn, U., Snyder, G.T., Muramatsu, Y., 2007b. Iodine as a tracer of organic material: 129I results from gas hydrate systems and fore arc fluids. J. Geochem. Explor. 95, 66–80.
Franklin, J.M., Gibson, H.L., Jonasson, I.R., Galley, A.G., 2005. Volcanogenic massive sulfide deposits. Econ. Geol. 100th Anniversary, 523–560.
Freyssinet, Ph., Butt, C.R.M., Morris, R.C., 2005. Ore-forming processes related to lateritic weathering. Econ. Geol. 100th Anniversary, 681–722.
Gammons, C.H., Yu, Y., 1997. The stability of aqueous silver bromide and iodine complexes at 25-300°C. Experiments, theory and geologic applications. Chem. Geol. 137, 155–173.
Gillard, R.D., Hart, A.D., Humphreys, D.A., Symes, R.F., Williams, P.A., 1997. Compositions of silver halides from the Brocken Hill district, New South Wales. Rec. Aust. Mus. 49, 217–228.
Golebiowska, B., Pieczka, A., Rzepa, G., Matyszkiewicz, J., Krajewski, M., 2010. Iodargyrite from Zalas (Cracow area, Poland) as an indicator of Oligocene-Miocene aridity in Central Europe. Palaeogeogr. Palaeoclimatol. 296, 130–137.
Gray, D.J., Butt, C.R.M., Lawrance, L.M., 1992. The geochemistry of gold in lateritic environments. In: Butt, C.M.R., Zeegers, H. (Eds.), Regolith exploration geochemistry in tropical and sub-tropical terrains. Hand-book of exploration geochemistry 4, pp. 461–482.
Harvey, G.R., 1980. A study of the chemistry of iodine and bromine in marine sediments. Mar. Chem. 8, 327–332.
Hem, J.D., 1985. Aluminum species in water. In: Baker, A.R. (Ed.), Trace Inorganics in Water. Am. Chem. Sot., Adv. Chem. Ser. 73, pp. 98–114.
Hill, P.J., 1958. Banded pyrite deposits of minas Carlota, Cuba. Econ. Geol. 53, 966–1003.
Horan, S.L., 1995. The geochemistry and tectonic significance of the Maimón-Amina schist's, Cordillera Central, Dominican Republic. Unpublished M.S. thesis, University of Florida, Gainesville, 172 pp.
Hu, Q., Zhao, P., Moran, J.E., Seaman, J.C., 2005. Sorption and transport of iodine species in sediments from the Savannah River and Hanford Sites. J. Contam. Hydrol. 78, 185–205.
Izawa, M.R.M., Shuster, J., Banerjee, N.R., Flemming, R.L., Southam, G., 2010. Microbes influence the mobilization and re-precipitation of Ag in gossans. Goldschmidt Conf. Abs. p. A450.

Karasyova, O.N., Ivanova, L.I., Lakshtanov, L.Z., 1998. Complexation of Gold(III)-chloride at the surface of hematite. Aquat. Chem. 4, 215–231.
Kennedy, H.A., Elderfield, H., 1987a. Iodine diagenesis in non-pelagic deep-seasediments. Geochim. Cosmochim. Acta 51, 2505–2514.
Kennedy, H.A., Elderfield, H., 1987b. Iodine diagenesis in pelagic deep-sea sediments. Geochim. Cosmochim. Acta 51, 2489–2504.
Keppler, F., Biester, H., Putschew, A., Silk, P.J., Schöler, H.F., Müller, G., 2004. Organoiodine formation during humidification in peatlands. Environ. Chem. Lett. 1, 219–223.
Kesler, S., Russell, E.N., Reyes, C., Santos, L., Rodriguez, A., Fondeur, L., 1991. Geology of the Maimon Formation, Dominican Republic. In: Mann, P., Draper, G., Lewis, J.F. (Eds.), Geologic and tectonic development of the North America-Caribbean plate boundary in Hispaniola. Geol. S. Am. S 262, pp. 173–185.
Kesler, S.E., Campbell, I.H., Allen, C.M., 2005. Age of the Los Ranchos Formation, Dominican Republic: Timing and tectonic setting of primitive island arc volcanism in the Caribbean region. Geol. Soc. Am. Bull. 117, 987–995.
Kojima, S., Astudillo, J., Rojo, J., Tristá, D., Hayashi, K., 2003. Ore mineralogy, fluid inclusion, and stable isotopic characteristics of stratiform copper deposits in the Coastal Cordillera of northern Chile. Miner. Deposita 38, 208–216.
Laznicka, P., 1988. Breccia and coarse fragmentites, petrology, environments, associations, ores. Developments in Economic Geology 25. Elsevier, Amsterdam (832 pp.).
Laznicka, P., 1989. Breccia and ores. Part 1: History, organization and petrography of breccias. Ore Geol. Rev. 4, 315–344.
Lengke, M.F., Southam, G., 2007. The deposition of elemental gold from gold(I)-thiosulfate complexes mediated by sulfate-reducing bacterial conditions. Econ. Geol. 102, 109–126.
Lewis, J.F., Draper, G., 1990. Geology and tectonic evolution of the Northern Caribbean margin. In: Dengo, G., Case, J.E. (Eds.), The Caribbean region. Boulder, ColoradoGeol. Soc. Am. The Geology of North America H, pp. 77–140.
Lewis, J.F., Astacio, V.A., Espaillat, J., Jiménez, J., 2000. The occurrence of volcanogenic massive sulfide deposits in the Maimón Formation, Dominican Republic. In: Sherlock, R., Logan, M.A.V. (Eds.), VMS Deposits of Latin America. Geol. Assoc. of Canada Spec. Publ. 2, pp. 213–239.
Lewis, J.F., Escuder Viruete, J., Hernaiz Huerta, P.P., Gutiérrez, G., Draper, G., 2002. Subdivisión geoquímica del arco de isla Circum-Caribeño, Cordillera Central Dominicana: implicaciones para la formación, acreción y crecimiento cortical en un ambiente intraoceánico. Acta Geol. Hisp. 37, 81–122.
Lewis, J.F., Draper, G., Proenza, J.A., Espaillat, J., Jiménez, J., 2006. Ophiolite-related ultramafic rocks (serpentinites) in the Caribbean region: a review of the occurrence, composition, origin, emplacement and Ni-laterite soil formation. Geol. Acta 4, 237–263.
Mann, A.W., 1984. Mobility of gold and silver in lateritic weathering profiles: some observations from Western Australia. Econ. Geol. 79, 38–49.
Mann, P., Draper, G., Lewis, J.F., 1991. An overview of the geologic and tectonic development of Española. In: Mann, P., Draper, G., Lewis, J.F. (Eds.), Geologic and tectonic development of the North-America–Caribbean plate boundary in española. Geol. Soc. Am. Spec. Spec. Paper 262, pp. 1–28.
Martín, M., Draper, G., 1999. Mapa geológico de la hoja 6172-I (Hatillo) a escala 1:50 000 (SYSMIN, Proyecto C). Consorcio ITGE-PROINTEC-INYPSA. Dirección General de Minería, Santo Domingo.
Millsteed, P.W., 1998. Marshite-miersite solid solution and iodargyrite from Broken Hill, New South Wales, Australia. Mineral. Mag. 62, 471–475.
Moran, J.E., Teng, R.T.D., Rao, U., Fehn, U., 1995. Detection of iodine in geologic materials by high-performance liquid chromatography. J. Chromatogr. 706, 215–220.
Moran, J.E., Oktay, S., Santschi, P.H., Schink, D., 1999. Atmospheric dispersal of 129I from nuclear fuel reprocessing facilities. Environ. Sci. Technol. 33, 2536–2542.
Muramatsu, Y., Wedepohl, K.H., 1998. The distribution of iodine in the Earth's crust. Chem. Geol. 147, 201–216.
Muramatsu, Y., Fehn, U., Yoshida, S., 2001. Recycling of iodine in fore-arc areas: Evidence from the iodine brines in Chiba, Japan. Earth Planet. Sci. Lett. 192, 583–593.
Muramatsu, Y., Yoshida, S., Fehn, U., Amachi, S., Ohmomo, Y., 2004. Studies with natural and anthropogenic iodine isotopes: iodine distribution and cycling in the global environment. J. Environ. Radioact. 74, 221–232.
Nahon, D.B., Boulangé, B., Colin, F., 1992. Metalogeny of weathering: an introduction. In: Weathering sols and paleosols. In: Martini, I.P., Chesworth, W. (Eds.), Developments in earth surface processes 2. Elsevier, pp. 445–471.
Nelson, C.E., Proenza, J.A., Lewis, J.F., López-Kramer, J., 2011. The metalogenic evolution of the Greater Antilles. Geol. Acta 9, 229–264.
Osborn, S.G., McIntosh, J.C., Hanor, J.S., Biddulph, D., 2012. Iodine-129, $^{87}Sr/^{86}Sr$, and trace elemental geochemistry of northern Appalachian basin brines: evidence for basinal-scale fluid migration and clay mineral diagenesis. Am. J. Sci. 312, 263–287.
Palacios, C., Guerra, N., Townley, B., Lahsen, A., Parada, M., 2005. Copper geochemistry in salt from evaporite soils, Coastal Range of the Atacama Desert, northern Chile: an exploration tool for blind Cu deposits. Geochem. Explor. Environ. Anal. 6, 371–378.
Pekov, I.V., Lykova, I.S., Bryzgalov, I.A., Ksenofontov, D.A., Zyryanova, L.A., Litvinov, N.D., 2011. Uniquely high-grade iodine mineralization in the oxidation zone of the Rubtsovskoe base-metal deposit, Northwest Altai, Russia. Geol. Ore Deposits 53, 683–698.
Penrose, R.A.F., 1894. The surficial alteration of ore deposits. J. Geol. 2, 288–317.
Pérez-Estaún, A., Hernaiz Huerta, P.P., Lopera, E., Joubert, M., Escuder-Viruete, J., Díaz de Neira, A., Monthel, J., García-Senz, J., Ubrien, P., Contreras, F., Bernárdez, E., Stein, G., Deschamps, I., García-Lobón, J.L., Ayala, C., 2007. Geología de la República Dominicana: de la construcción del arco-isla a la colisión arco-continente. Bol. Geol. Min. 118, 157–174.
Pindell, J.K., Barrett, S.F., 1990. Geological evolution of the Caribbean region: A plate-tectonic Caribbean Region. Geol. Soc. Am. Geology of North America H, pp. 405–432.
Price, N.B., Calvert, S.E., 1973. The geochemistry of iodine in oxidised and reducedrecent marine sediments. Geochim. Cosmochim. Acta 37, 2149–2158.
Proenza, J.A., Zaccarini, F., Lewis, J.F., Longo, F., Garuti, G., 2007. Chromian spinel composition and the platinum-group minerals of the PGE-rich Loma Peguera chromitites, Loma Caribe peridotite, Dominican Republic. Can. Mineral. 45, 631–648.
Prospero, J.M., Mayol-Bracero, O.L., 2014. Understanding the transport and impact of African dust on the Caribbean basin. Bull. Am. Meteorol. Soc. http://dx.doi.org/10.1175/BAMS-D-12-00142.1 (in press). Q9
Puigdomènech, I., 2010. MEDUSA (Make Equilibrium Diagrams Using Sophisticated Algorithms) Windows interface to the MS-DOS versions of INPUT, SED and PREDOM (FORTRAN programs drawing chemical equilibrium diagrams) Vers. 6 Dec 2010. Royal Institute of Technology, Stockholm, Sweden.
Ran, Y., Fu, J., Rate, A.W., Gilkes, R.J., 2002. Adsorption of Au(I, III) complexes on Fe, Mn oxides and humic acid. Chem. Geol. 185, 33–49.
Reich, M., Chryssoulis, S., Palacios, C., 2008. Nanoscale mineralogy of Ag in sulfides from Cu deposits in northern Chile: Implications for ore genesis, exploration and metallurgical recovery. Geochim. Cosmochim. Acta 72, 783.
Reich, M., Palacios, C., Alvear, M., Cameron, E.M., Leybourne, M.I., Deditius, A., 2009. Iodine-rich waters involved in supergene enrichment of the Mantos de la Luna argentiferous copper deposit, Atacama Desert, Chile. Miner. Deposita 44, 719–722.
Reich, M., Snyder, G.T., Alvarez, F., Pérez, A., Palacios, C., Vargas, G., Cameron, E.M., Muramatsu, Y., Fehn, U., 2013. Using iodine isotopes to constrain supergene fluid sources in arid regions: insights from the Chuquicamata oxide blanket. Econ. Geol. 108, 163–171.
Reith, F., Rogers, S.L., McPhail, D.C., Webb, D., 2006. Biomineralization of gold: biofilms on bacterioform gold. Science 313, 233–236.
Roca, A., Arranz, J.V.M., Calero, J., 1999. Characterization and alkaline decomposition/cyanidation of beudantite-jarosite materials from Rio Tinto gossan ores. Can. Metall. Q. 38, 93–103.
Schwertmann, U., Murad, E., 1983. Effect of pH on the formation of goethite and hematite from ferrihydrite. Clay Clay Miner. 31, 277–284.
Scholz, F., Hnesen, C., Lu, Z., Fehn, U., 2010. Controls on the $^{129}I/I$ ratio of deep-seated marine interstitial fluids: 'Old' organic versus fissiogenic 129-iodine. Earth Planet. Sci. Lett. 294, 27–36.
Scott, K.M., Ashley, P.M., Lawie, D.C., 2001. The geochemistry, mineralogy and maturity of gossans derived from volcanogenic Zn-Pb-Cu deposits in the eastern Lachlan Fold Belt, NSW, Australia. J. Geochem. Explor. 72, 169–191.
Shacketon, N.J., 1978. Evolution of the Earth's climate during the Tertiary era. In: Gauter, D. (Ed.), International conference on evolution of planetary atmospheres and climatology of the earth. Centre National d'Études Spatiales, France, pp. 49–58.
Sillitoe, R.H., 2009. Supergene silver enrichment reassessed. In: Titley, S.R. (Ed.), Supergene environments and products. Society of Economic Geologists, Spec. Pub. 14, pp. 15–32.
Sillitoe, R.H., Clark, A.H., 1969. Copper and copper-iron sulfides as the initial products of supergene oxidation, Copiaó Mining district, Northern Chile. Am. Mineral. 54, 1680–1710.
Six, J., Feller, C., Denef, K., Ogle, S.M., Moraes Sa, J.C., Albrecht, A., 2002. Soil organic matter, biota and aggregation in temperate and tropical soils – effects of no-tillage. Agronomie 22, 755–775.
Smith, A.D., Hunt, R.J., 1985. Solubilisation of gold by *Chromobacterium violaceum*. J. Chem. Technol. Biotechnol. 35B, 110–116.
Stoffregen, R., 1986. Observations on the behavior of gold during supergene oxidation at Summitville, Colorado, U.S.A., and implications for electrum stability in the weathering environment. Appl. Geochem. 1, 546–558.
Swap, R., Garstang, M., Greco, S., Talbot, R., Kallberg, P., 1992. Saharan dust in the Amazon Basin. Tellus Ser. B 44 B, 133–149.
Taylor, R., 2011. Gossans and leached cappings: field assessment. Springer-Verlag Berlin Heidelberg, (146 pp.).
Taylor, G.F., Thornber, M.R., 1992. The mechanisms of sulfide oxidation and gossan formation. In: Butt, C.R.M., Zeegers, H. (Eds.), Regolith exploration geochemistry in tropical and subtropical terrainsHandbook of Exploration Geochemistry 4. Elsevier, Amsterdam, pp. 119–138.
Thornber, M.R., Taylor, G.F., 1992. Gossan and ironstone surveys. In: Butt, C.R.M., Zeegers, H. (Eds.), Regolith exploration geochemistry in tropical and subtropical terrainsHandbook of Exploration Geochemistry 4. Elsevier, Amsterdam, pp. 139–202.
Velasco, F., Herrero, J.M., Suárez, S., Yusta, I., Alvaro, A., Tornos, F., 2013. Supergene features and evolution of gossans capping massive sulfide deposits in the Iberian Pyrite Belt. Ore Geol. Rev. 53, 191–203.
Viñals, J., Roca, A., Cruells, M., Nunez, C., 1995. Characterization and cyanidation of Rio-Tinto gossan ores. Can. Metall. Q. 34, 115–122.
Viñals, J., Roca, A., Arranz, M., 2003. Autoclave alkaline decomposition and cyanidation of jarosite-beudantite phases from Rio Tinto gossan ores. Can. Metall. Q. 42, 29–40.
Watkins, J., 1990. Geologic Setting of the Cerro de Maimón Deposit, Dominican Republic. Geologic report for Falconbridge Dominicana, Santo Domingo (43 pp.).
Watterson, J.R., 1991. Primary evidence for the involvement of budding bacteria in the origin of Alaskan placer gold. Geology 20, 315–318.
Webster, J.G., Mann, A.W., 1984. The influence of climate, geomorphology and primary geology on the supergene migration of gold and silver. J. Geochem. Explor. 22, 21–42.
Whiterhead, W.L., 1919. The veins of Chañarcillo, Chile. Econ. Geol. 14, 1–45.
Williams, D., 1950. Gossanized breccia-ores, jarosites and jaspers at Rio Tinto, Spain. Bull. Inst. Min. Metall. 526, 1–12.
Yesares, L., Sáez, R., Nieto, J.M., Ruiz de Almodóvar, G., Cooper, S., 2014. Supergene enrichment of precious metals by natural amalgamation in the Las Cruces weathering profile (Iberian Pyrite Belt, SW Spain). Ore Geol. Rev. 58, 14–26.
Zhang, Y., Fang, Z., Muhammed, M., 1997. On the solution chemistry of cyanidation of gold and silver bearing sulfide ores.A critical evaluation of thermodynamic calculations. Hydrometallurgy 46, 251–269.

Please cite this article as: Andreu, E., et al., Weathering profile of the Cerro de Maimón VMS deposit (Dominican Republic): textures, mineralogy, gossan evolution and mobility of..., Ore Geol. Rev. (2014), http://dx.doi.org/10.1016/j.oregeorev.2014.09.015